

SHEAR STRENGTHENING OF RC BEAM USING FRP

A DISSERTATION

*Submitted a partial fulfilment of the
requirement for the award of the degree
of*

MASTER OF TECHNOLOGY

in

CIVIL ENGINEERING

(With specialization in Structural Engineering)

By

**PAVAN KUMAR MEENA
(17523017)**



DEPARTMENT OF CIVIL ENGINEERING

INDIAN INSTITUTE OF TECHNOLOGY ROORKEE

ROORKEE -247667 (INDIA)

MAY, 2019

CANDIDATE'S DECLARATION

It is certified that this work has been carried out in the department of civil engineering at Indian institute of Technology, Roorkee under the Supervision of Dr. Anupam Chakrabarti, Professor in Structural Engineering Group, Department of Civil Engineering, IIT Roorkee (India).

Place: Roorkee

Date: May, 2019

(PAVAN KUMAR MEENA)

DEPARTMENT OF CIVIL ENGINEERING

INDIAN INSTITUTE OF TECHNOLOGY

ROORKEE (INDIA)

May 2019



Certificate

This is to certify that this thesis entitled “**SHEAR STRENGTHENING OF R.C. BEAM USING FRP**” is a bonafide record (Thesis) presented by **PAVAN KUMAR MEENA** towards the partial fulfilment of the requirements for the award of M-Tech and correct to the best of my knowledge.

Dr Anupam Chakrabarti
Professor
Indian institute of Technology
Roorkee (247667)

ACKNOWLEDGEMENT

I wish to express my most sincere appreciation and gratitude to **Dr Anupam Chakrabarti** (Professor), Structural Engineering, Department of Civil Engineering, Indian Institute of Technology, Roorkee for his valuable guidance and continuous encouragement during preparation of this thesis work.

Place: IIT Roorkee

Date: May, 2019

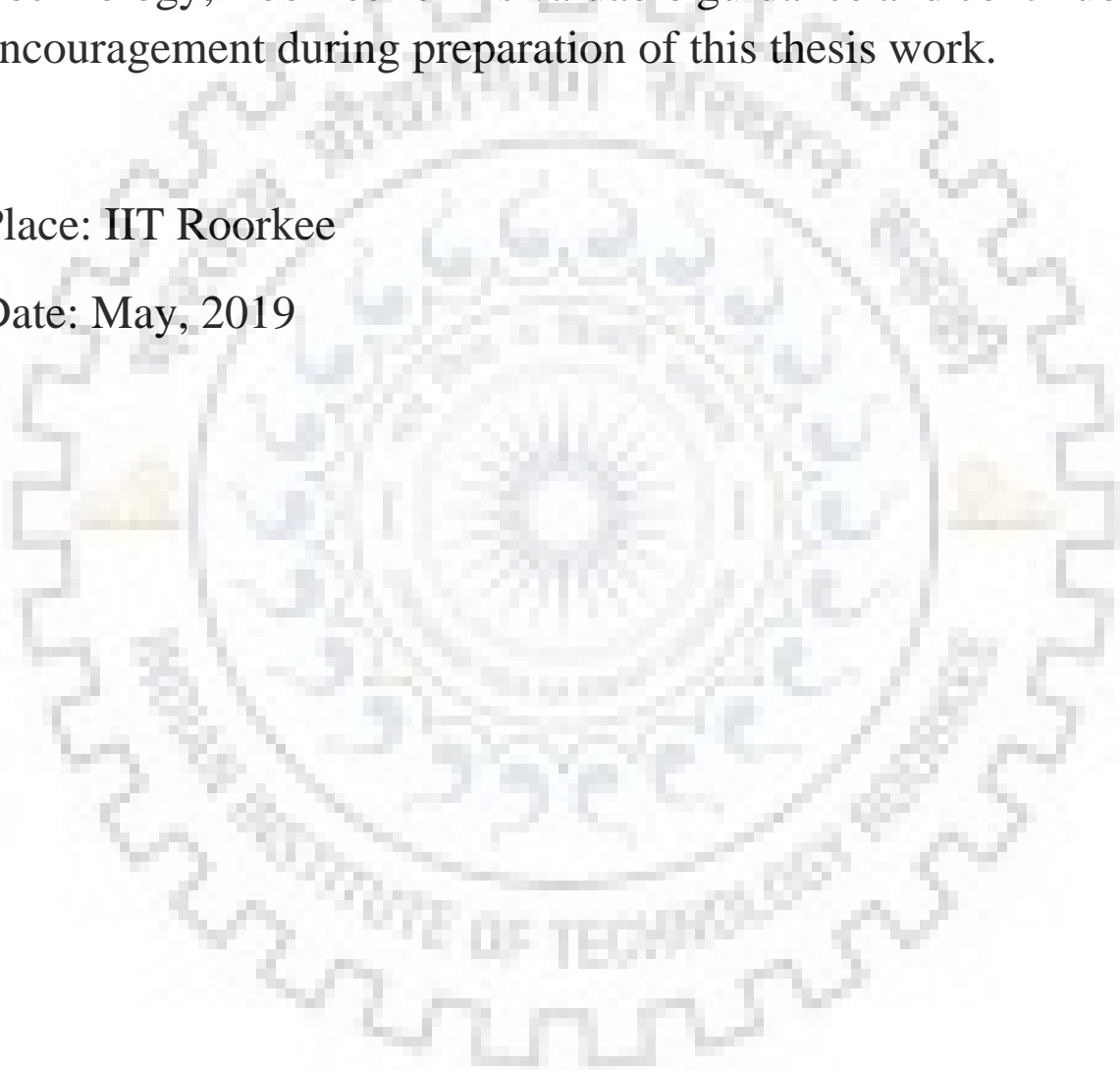


TABLE OF CONTENTS

CONTENTS	PAGE NO.
<i>Candidate's declaration</i>	<i>i</i>
<i>Certificate</i>	<i>ii</i>
<i>Acknowledgement</i>	<i>iii</i>
<i>Table of contents</i>	<i>iv</i>
<i>Abstract</i>	<i>vi</i>
<i>List of figures</i>	<i>vii</i>
<i>List of tables</i>	<i>x</i>
CHAPTER-1: INTRODUCTION	1-4
1.1 Background	1
1.2 Aim and Scope	1
1.3 Fibre Reinforced Polymer (FRP)	2
1.4 Research Approach	4
CHAPTER-2: LITERATURE REVIEW	5-8
2.1 General	5
2.2 Shear strengthening various techniques	5
2.3 Strengthening with FRP composites	5
CHAPTER-3: ANALYTICAL WORK ON RC BEAM USING CFRP	9-12
CHAPTER-4: NUMERICAL SOLUTION FOR RC BEAM	13-27
4.1 Shear Test Specimen used for experiment	13
4.2 Numerical model and materials properties	15
4.2.1 Beam models studied	15
4.2.2 Material models	17
4.2.2.1 Concretes	17
4.2.2.2 Steel	19
4.2.2.3 FRP material	20
4.2.3 Modelling of FRP- concrete interface	22
4.2.4 Meshing and modelling	23

4.3 Meshing and Modelling	23
CHAPTER- 5: RESULTS AND DISCUSSIONS	28-46
5.1 Introduction	28
5.2 Convergence study of FEM model	28
5.2.1 Control beam	28
5.2.2 Strengthened beam	29
5.3 Validation of Results	32
5.3.1 Control beam	32
5.3.2 Retrofitted beam	32
5.4 Parametric study	36
5.4.1 Effect of different types of FRP's with respect to different heights	36
5.4.2 Orientation effects of CFRP	39
5.4.3 Effects in shear behaviour change in percentage tension reinforcement	45
CHAPTER- 6: CONCLUSION AND RECOMMENDATIONS	47-48
6.1 Conclusion	47
6.2 Scope of future works	48
REFERENCE	

ABSTRACT

Many factors in service life which may be natural or manmade, are affecting existing concrete building structures. Corrosion of bars, spalling and deterioration of concrete and earthquake affect its performance of resisting loads, which lead to failure. Hence to prevent it from sudden failure FRP is one of the best materials for strengthening. FRP provides high strength and lightweight, corrosion resistance, nonconductive and impact resistant properties.

This thesis has presented some literature review on failure behaviour of RC beam under shear strengthening. The scope of work has been identified based on the above review work. The commercial FEM software, **ABAQUS-2017** has been used for the purpose of implementing the works.

The objectives of this study were to investigate the behaviour of retrofitted beams and to develop a finite element model for FRP strengthened beams having different varying design parameters. The finite element model has been verified with other experimental and analytic results. Finally, the influence of different parameters on the behaviour of the strengthened beams was investigated. In this model non-linear behaviour of concrete material has been studied.

A mesh convergence study has been conducted to choose suitable number of elements for getting accurate results. Then some parametric studies were conducted for different types of FRP, orientations of FRP, different lengths of FRP and percentage of tensile reinforcement taking into account the shear behaviour of RC beam. Different types of FRP such as CFRP, E-GFRP and BFRP have also been considered to see their effect on shear capacity of beam.

The variation of strength in terms of load and deflection has been studied in case of perfect bonding with single and composite layer of FRP. Tension damage failure of concrete was also studied.

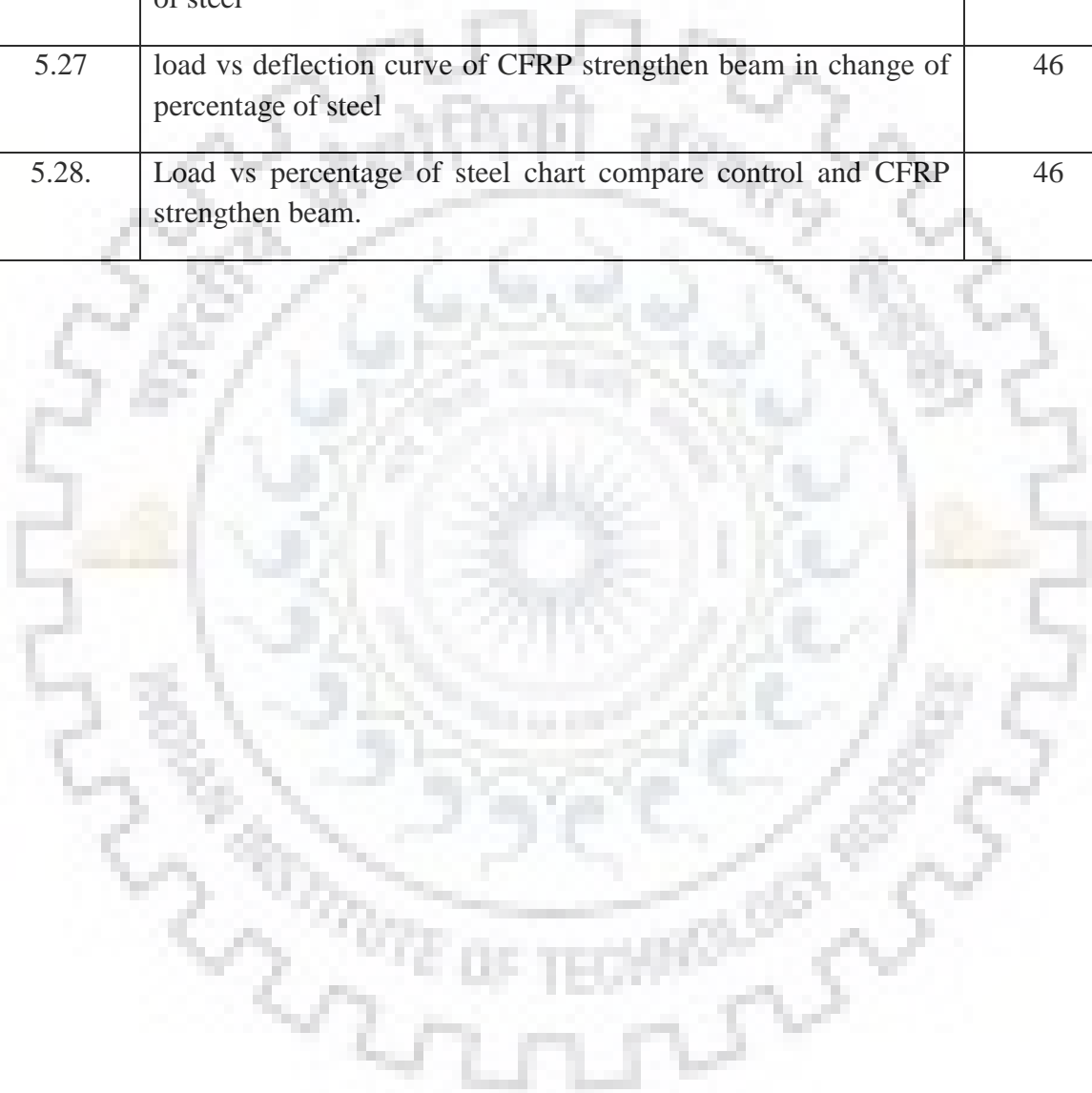
The results showed that when the length of FRP increased the load capacity of the beam also increased due to shear strengthening. Increased CFRP stiffness increased the maximum load only up to a certain value of the stiffness, and there after the maximum load decreased.

LIST OF FIGURES

Fig. No.	Description	Page No.
1.1	Types of FRP composites	2
1.2	A schematic diagram showing a typical unidirectional FRP plate	2
1.3	The unidirectional fiber sheets (a) basalt fiber sheet (b) carbon fiber sheet (c) E-glass fiber sheet	3
2.1	FRP shear strengthening schemes	6
2.2	Rip-off failure of control beam	6
2.3	Peel-off failure of the strengthening beam	6
2.4	Supports, loading and position of LVDT	7
2.5	Size and positioning of beams and reinforcements in groups RF and RS	7
3.1	Reinforcement and cross-section distribution	9
3.2	Strain and stress distribution of beam	9
4.1	Geometry and reinforcement of beam.	13
4.2	Loading, supports and LVDT's position	14
4.3	Arrangement of CFRP laminate in retrofitted beams.	14
4.4	Experimental setup	16
4.5	Stress strain behaviour of concrete under uniaxial compression	18
4.6	Concrete under uniaxial tension	19
4.7	Stress strain behaviour of steel	19
4.8	Model of concrete beam with reinforcement	20
4.9	Elastic brittle fibre & Elastic-plastic Matrix	20
4.10	Bilinear traction–separation constitutive law.	22
4.11	4-Node linear tetrahedral element.	23
4.12	One quarter of beam using symmetry	24

4.13	Boundary conditions	24
4.14	Model boundary condition	25
4.15	Orientation of fibres in each composite layup	25
4.16	Finite element mesh of a quarter of control & strengthened beam	26
5.1	Control beam yield behaviour in shear direction.	29
5.2	Mesh convergence of control beam	29
5.3	Load vs deflection curve for different mesh size of strengthening beam	30
5.4	Graphical result of solid layer of FRP	30
5.5	Graphical result of shell layer of FRP	31
5.6	Strengthening beam yield behaviour in shear direction	31
5.7	Load vs Deflection curve of Control beam	32
5.8	Load vs Deflection curve of Retrofitted beam	33
5.9	Deflection of retrofitted Quarter beam	33
5.10	Tension damage control beam	34
5.11	Compression damage control beam	34
5.12	Compression damage of strengthening beam	35
5.13	Tension damage strengthening beam	35
5.14	Load v/s deflection curve of CFRP	36
5.15	Load v/s deflection curve of BFRP	37
5.16	Load v/s deflection curve of E-GFRP	37
5.17	Load v/s height curve of FRP with different type.	38
5.18	Different heights of CFRP	38
5.19	Load vs deflection curve at 300mm height	39
5.20	Load vs deflection curve at 200mm height	40
5.21	Load vs deflection curve at 150mm height	40

5.22	Load vs deflection curve at 100mm height	40
5.23	Load vs height of different orientation	41
5.24(A-E)	Tresca stress variation of CFRP laminate at 90 ⁰ orientation.	43
5.25(A-E)	Tresca stress variation of CFRP laminate at 45 ⁰ orientation.	44
5.26	load vs deflection curve of control beam in change of percentage of steel	45
5.27	load vs deflection curve of CFRP strengthen beam in change of percentage of steel	46
5.28.	Load vs percentage of steel chart compare control and CFRP strengthen beam.	46



LIST OF TABLES

Table No.	Description	Page No.
1.1	Strength and stiffness value for material used in retrofiting	4
4.1	Mechanical properties of materials used.	14
4.2	Mechanical properties of FRP	21
4.3	Number of elements, nodes, variable and CPU time of Different Models.	26
5.1	Load and deflection values	28
5.2	Load and deflection values different Mesh	29
5.3	Convergence result of different FRP construction type	30
5.4	Load vs deflection data of CFRP	36
5.5	Load vs deflection data of BFRP and E-GFRP	36
5.6	Load vs deflection values with different height	39
5.7	Load vs deflection values in change of percentage of tension reinforcement	45

Chapter-1

Introduction

1.1 Background

FRP was introduced in 1940s and today it is used in different fields from aerospace to civil engineering. It has decent properties than other materials. Usage of FRP in RCC structure modifies and improves the performance as well as duration of structure in its lifetime. FRP was generally used for changing structural purpose, new structure construction, deterioration of reinforcing steel due to corrosion and an unfortunate incident such as earthquakes.

In such domain there are two prospective aspects: one is replacement another is retrofitting. Complete replacement of structure was difficult because of increased cost for material and labour and transportation charges e.g. machinery adjustment space, traffic problems. So, it is usually advisable to repair the structure.

In the last decade, excess uses of epoxy and fibre resin form laminate. Laminate is form of different sheets, plates, FRP bar and prefabricated shell has been noted. These were bonded at the outer surface of concrete, but in case of FRP bars these could also be grouted by NSM technique.

FRP is one of the best materials as compared to traditional steel plates in following prospect. FRP has high strength and low-density ratio, corrosion resistant, have high impact resistance and installation process is easier and temporary support until the strength gains is not required because of low weight. In this thesis, study is involved of shear strengthening of reinforcement concrete beam with externally bonded FRP laminates using FEM software ABAQUS.

1.2 Aim and Scope

The overall objective of current study is to analysis and improve the understanding of the behaviour of RC beam strength with FRP in shear failure and compare FEM result with experimental results.

Beam has been tested in four-point loading test until shear failure crack is developed. The ABAQUS program is use to develop FEM models for simulation and draw load-deflection relationship until failure. Generate relation of strength with different type of FRP, change orientation of FRP laminate, different length of FRP layer and change percentage of steel in tension.

1.3 Fibre Reinforced Polymer (FRP)

FRP is the best composite material that developed into economically and structurally construction materials for building and bridge. It consists of a matrix of fibres and polymer resin. Here epoxy, polyester, vinyl ester or phenolic thermosetting resin which have fibres concentration ratio is greater than 30% by volume. The polymer composites shown in flow diagram Fig.1.1

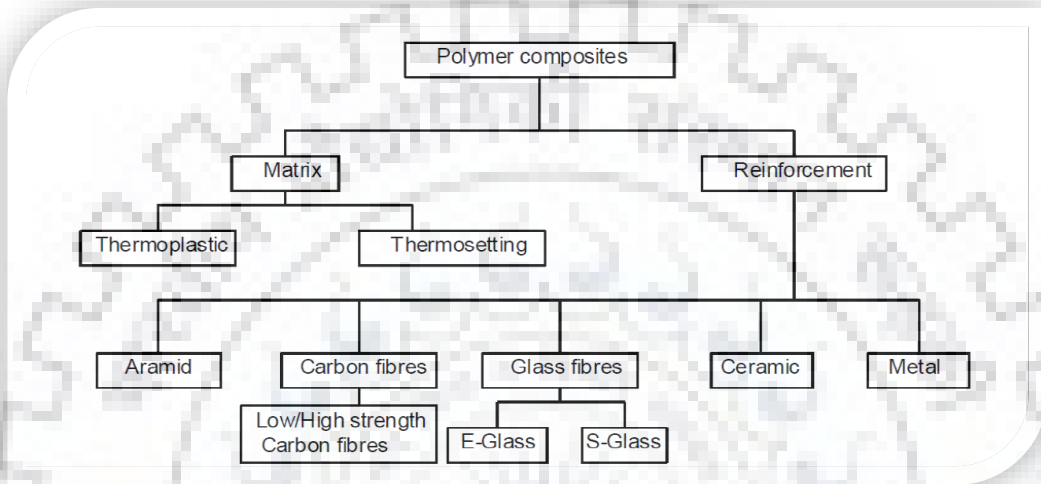


Fig.1.1: Types of FRP composites

Fibres show linear elastic behaviour up to failure and do not give significant yielding as compare to steel. The initial function of matrix in a composite is to transfer stress between the fibres. Generally mechanical properties of composites depend upon fibres orientation, fibres properties, volume fraction and also depend on properties of polymer resins. If fibres are orientated in one direction, it is known as unidirectional and if fibres orientated in many directions is known as bi-directional or multi-directional shown in Fig. 1.2.

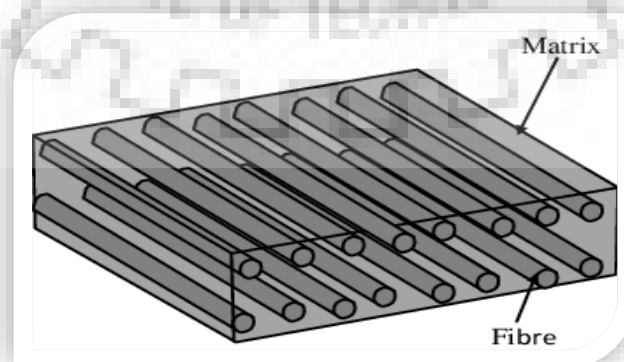


Fig. 1.2: A schematic diagram showing a typical unidirectional FRP plate

Attach the FRP laminate to other surface such as concrete using adhesives. Most popular adhesive used are **Acrylics, Epoxies and Urethanes**. Properties of epoxy are highly bond strength and high temperature resistance, whereas acrylics give moderate temperature resistance, good strength and rapid curing. Adhesive bond effectively works on good surface preparation like removing cement paste and duct generated by surface grinding using air blower and carefully curing.

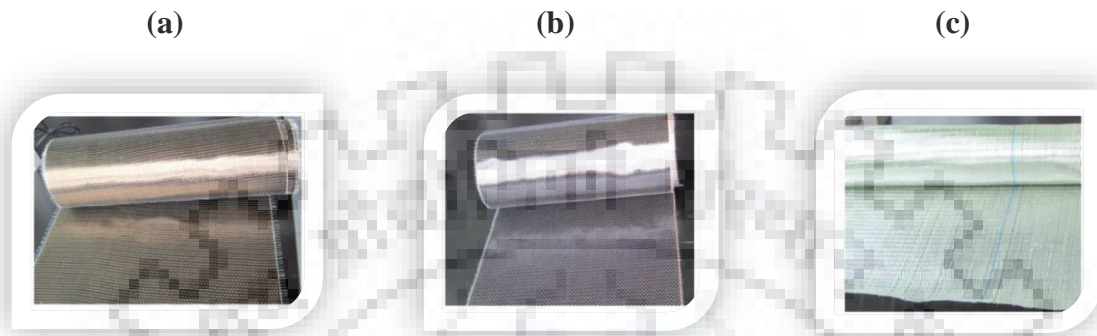


Fig. 1.3: The unidirectional fiber sheets (a) Basalt fiber sheet (b) Carbon fiber sheet (c) E-glass fiber sheet

The advantages of BFRP mainly eco-friendly properties because the basalt fibre can be obtained directly from natural resources such as in molten volcanic rocks. When GFRP composites compared to BFRP, it possesses a higher strength and modulus at a comparable cost while offering greater chemical stability. In addition, the superior creep behaviour of BFRP allows its efficient usage in pre-stressing applications than GFRP. When compared to CFRP and BFRP, it's possesses a very similar high temperature working ability at a reduced cost and thus making BFRP is a strong competitor in various applications. Different types of FRP laminates are shown in above Fig. 1.3.

The approximate stiffness and strength of a unidirectional CFRP with a 65% volume fraction of carbon fibres and 50-70% volume fraction of GFRP, BFRP is given in Table 1.1 comparing with steel. Epoxy is usually used as adhesive, which transfers the load to fibres when load is provided and provide also durability.

Table 1.1 Strength and stiffness value for material used in retrofitting.

Material	Tensile strength (M Pa)	Modulus of elasticity (G Pa)	Density (kg/m ³)	Modulus of elasticity to density ratio (Mm ² /s ²)
Carbon	2200-5600	240-830	1800-2200	130-380
Aramid	2400-3600	130-160	1400-1500	90-110
Glass	3400-4800	70-90	2200-2500	31-33
Epoxy	60	2.5	110-1400	1.8-2.3
CFRP	1500-3700	160-540	1400-1700	110-320
Steel	280-1900	190-210	7900	24-27
GFRP	480-1600	35-51	1570-2170	23-24
BFRP	1035-1650	45-59	1850-2240	25-27

1.4 Research Approach

In this session a three-dimensional finite element model was created in **ABAQUS/Standard explicit section**. This model has been validated with published experimental results and important issues here are materials properties, mesh convergence, element types, boundary condition, interface between materials and part type.

To evaluate the behaviour of concrete, following methodologies are available in ABAQUS.

1. Smearred crack model
2. Concrete damage plastic.

Here a CDP model has been chosen for study due to higher chance of convergence and another reason was here that stress-strain curve of concrete is defined in an exact way and CDP model assumes that the uniaxial tensile and compressive response of concrete as per damaged plasticity.

Chapter-2

Literature Review

2.1 General

Lots of works have been completed in the field of shear failure of reinforced concrete beam with steel plate, FRP strip and FRP plate. Major work is mostly done using experiments and very few researches have been done with numerical modelling using FEM software.

The following chapter presents some literature review of shear strengthened of RC beam using steel plate and different FRP plates using experimental, numerical and analytic calculations.

2.2 Shear strengthening by various techniques

Adhikary and Mutsuyoshi (2004) in this paper represented results of an experimental works for enhancing the shear capacity of RC beam with various method. Here eleven beams were considered in the test. They are divided in two series: first series were designed with failure modes as ductile and another was designed in brittle mode. Two beam kept control beam and other are strengthening with steel plates, steel brackets, vertical strips and externally anchored stirrups. In all these techniques, maximum load enhancing was found in **externally anchored stirrups** is 117% higher than the control beam at failure. And epoxy bonded steel plate 72% increase in shear strength as compare to control beam.

2.3 Strengthening with FRP composites

Khalifa et al. (2000) presented a conference paper of 27 RC beam model fail in shear strength with externally bonded CFRP in experimental works. Here three series of beams presenting: Series-A: - twelve full scale rectangular beam, Series-B: - full scale two span continuous rectangular beam is nine and Series-C: - full scale T-section RC beams six in number were strengthening with CFRP configuration. The following variables are studying with or without steel stirrups, CFRP amount and distribution, shear span to depth ratio, bonded side, fibre orientation and end anchor. All of variable coming results were increase shear span to depth ratio ($\frac{a}{d}$) increase the shear capacity, 45° orientation result is coming more as compare to 0°-90°, failure at average effective stress level below nominal strength due to stress concentration and debonding failure of CFRP from concrete surface and finally it's not important for increasing the CFRP, strength is increase because it's depended on bonding between concrete

and CFRP. In this experimental work enhancing shear capacity of RC beams in both negative and positive moment region.

There were two main mode of failure in shear strengthening of RC beam with FRP: FRP debonding and FRP rupture. **Chen and Tang (2003)** developing simple, accurate and rational design proposal for a shear capacity which was fail by FRP debonding. Here highlight shear strength deficiency and prepare new model and validated with the experimental data obtained from existing literature and finally presenting new design proposal. As shown in Fig 2.1 different FRP strengthening scheme used in Chen and Teng (2003) is presenting.

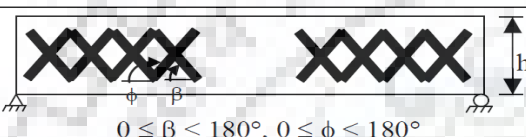


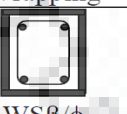
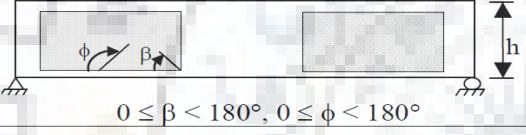

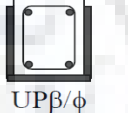

Fibre orientations	Bonding scheme and notation		
	Side	U jacket	Wrapping
 $0 \leq \beta < 180^\circ, 0 \leq \phi < 180^\circ$	 $SS\beta/\phi$	 $US\beta/\phi$	 $WS\beta/\phi$
 $0 \leq \beta < 180^\circ, 0 \leq \phi < 180^\circ$	 $SP\beta/\phi$	 $UP\beta/\phi$	 $WP\beta/\phi$

Fig. 2.1. FRP shear strengthening schemes

Serbescu et al. (2010) have represented experiments to show quality of basalt fibre (eco-friendly obtained by nature) as compare to expansive CFRP and less effective GFRP for shear strengthening of RC beam. In this paper BFRP can increase ultimate load capacity, anchorage and reduce brittleness of plate end debonding. It was found BFRP could be use as place to CFRP and it delays the failure of debonding and increases the durability. Failure mode of control beam was sudden concrete cover separation and shear strengthening beam is peeling off failure mode shown in Fig 2.2 and 2.3.

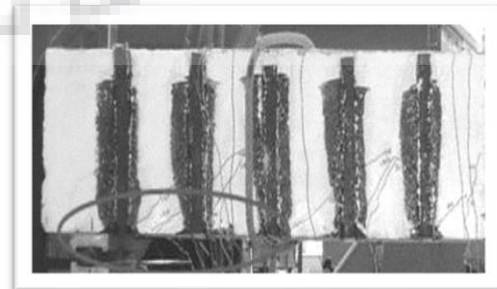
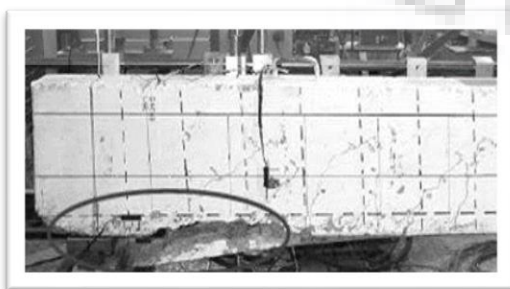


Fig 2.2 Rip-off failure of control beam Fig 2.3 Peel-off failure of the strengthening beam

Sundarraja et al. (2008) represented experimental work on GFRP. In this paper three sets of beams were tested first is control, second is two side GFRP and third is U-wrap. Aim-this paper was understanding the shear contribution of concrete, steel and additional capacity of GFRP. Conclusion-load deflection behaviour of U-wrap strip is better than side strip. And increase the width of GFRP and increasing shear contribution. In case of bonding vertical GFRP strips FRP rupture failure was more prominent then FRP debonding but in case of U-wrap crushing of concrete is more prominent.

Obaidat et al. (2010) investigated experimental works of flexure and shear strengthening of RC beam with carbon fibre laminate. Various parameters were taken in account such as CFRP length, laminate position, reinforcement ratio and testing twelve beams. Strength capacity was increasing when length of CFRP increasing in tension side. Debonding of CFRP laminates was main mode of failure and strengthening beam ultimate load capacity and stiffness was found to be more than control beam. Geometric and loading condition shown in Fig. 2.4 and 2.5(a, b) crack width for retrofitting beam is decreasing as compare to control beam. In shear strengthening load increase 23% and flexure strengthening between 7% - 33% increase as compare to control beam.

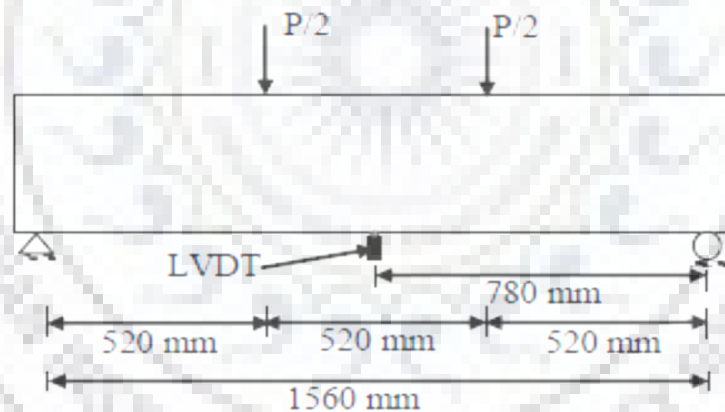
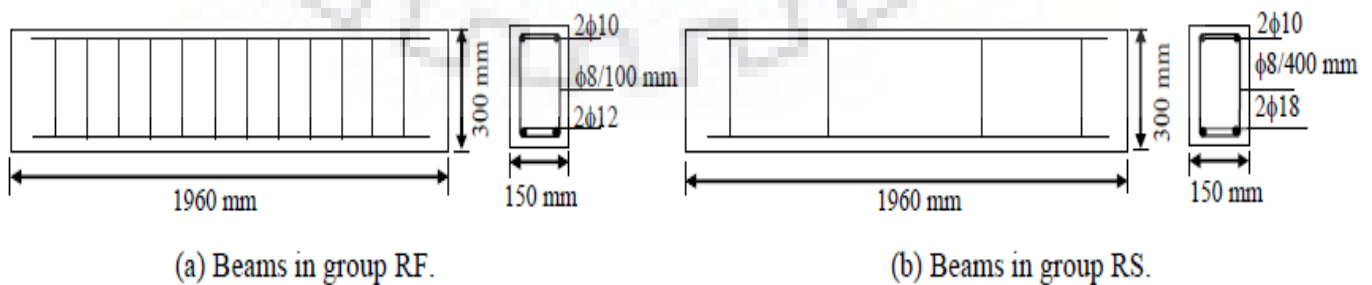


Fig. 2.4 Loading, supports, and position of LVDT



(a) Beams in group RF.

(b) Beams in group RS.

Fig. 2.5 Size and positioning of beams and reinforcements in groups RF and RS

Kharatmol et al. (2014) presented experimentally study between ultimate load carrying capacity and ductility of an RC beam and CFRP bonded in different pattern of flexure and shear capacity RC beam doing repair work. Here strength was increase 20%, 10.69% and 42.5% in case of tension side, 2-side and 3-side wrapped respectively.



Analytic Solution for RC beam using CFRP

In this section some examples of RC beams with FRP wrapping are solved by following some existing analytical solutions.

3.1 Given data

Total span length –	1960mm
Centre to centre span -	1560mm
Cylinder strength of concrete (f_c') -	30Mpa
Cube strength of concrete (f_{ck}) –	37.5Mpa
Flexure strength of steel (f_y)-	415Mpa
Thickness of CFRP strip (t_f) -	1.2mm
Width of CFRP strip (W_f) -	50mm
Elastic modulus of CFRP (E_{CFRP}) -	165Gpa
Stress in CFRP (f_{CFRP}) -	2Gpa

3.2 Reference for calculation

1. IS456-2000
2. ACI 440-2R 2017
3. Mitali and Gajjar (2012)

3.3 Beam configuration

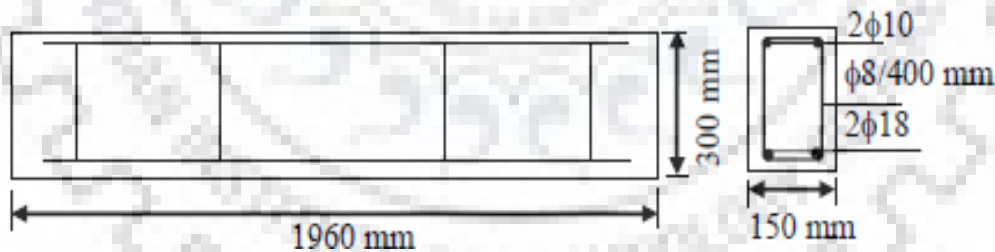


Fig. 3.1 Reinforcement and cross-section distribution

3.4 Depth of neutral axis

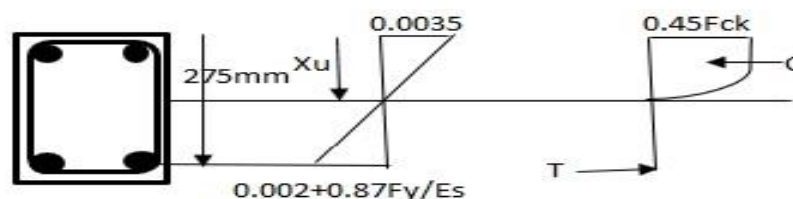


Fig. 3.2 Strain and stress distribution of beam.

$$C=T$$

$$0.36f_{ck}.bX_u = 0.87f_y A_{st} \quad \dots (3.1)$$

$$X_u = \frac{0.87 \cdot 415 \cdot 2 \cdot \frac{\pi}{4} \cdot 18^2}{0.36 \cdot 37.5 \cdot 150} = 90.74 \text{ mm}$$

$$\begin{aligned} X_{u \text{ lim.}} &= 0.48d \\ &= 0.48 \cdot 275 = 132 \text{ mm} \end{aligned}$$

Here $X_u < X_{u \text{ lim.}}$

So, section is under reinforcement.

3.5 Moment and Shear capacity of original section

$M_u = \text{Force} \times \text{Lever arm}$

$$= 0.87f_y \cdot A_{st} \cdot (d - 0.42X_u) \quad \dots (3.2)$$

$$= 0.87 \cdot 415 \cdot 2 \cdot \frac{\pi}{4} \cdot 18^2 \cdot (275 - 0.42 \cdot 90.74)$$

$$= 43.5288 \text{ KN-M}$$

Maximum shear force on original beam

$$\begin{aligned} V_{\text{org.}} &= \frac{M_u}{\text{Shear span}} \quad \dots (3.3) \\ &= \frac{43.5288}{0.52} = 83.709 \text{ KN} \end{aligned}$$

3.6 Shear capacity of strengthening beam

Here shears capacity taken by concrete, shear stirrups and CFRP strip.

a) **Shear capacity taken by Concrete:** -

Concrete capacity depends on τ_c so calculate -

$$\begin{aligned} \% \text{ of tension reinforcement} &= \frac{A_{st}}{bd} \cdot 100 \quad \dots (3.4) \\ &= \frac{2 \cdot \frac{\pi}{4} \cdot 18^2}{150 \cdot 275} \cdot 100 = 1.233\% \end{aligned}$$

Using interpolation find τ_c value in Table-19 (IS456-2000). It depends on grade of concrete (M37.5) and percentage of steel

Design shear strength of concrete (τ_c) = 0.73092 N/mm²

$$\tau_{c \text{ max}} = 3.827 \text{ N/mm}^2$$

$$\tau_c < \tau_{c \text{ max}} \quad \text{ok.}$$

Concrete taken shear

$$V_c = \tau_c \cdot bd \quad \dots (3.5)$$

$$=0.73092*150*275$$

$$=30.15 \text{ KN}$$

b) Shear capacity taken by stirrups

Design shear taken by vertical stirrups according to clause 40.4 (IS456-2000)

$$V_{us} = \frac{d}{S_v} A_{sv} \sigma_{sv} \quad \dots(3.6)$$

$$= \frac{275}{400} * 2 * \frac{\pi}{4} * 8^2 * 230$$

$$= 15.9 \text{ KN}$$

c) Total shear capacity original beam

$$V_{total} = V_c + V_{us} \quad \dots (3.7)$$

$$= 30.15 + 15.9$$

$$= 46.05 \text{ KN}$$

Excess shear

$$V_E = 83.709 - 46.05$$

$$= 37.659 \text{ KN}$$

For 2-side CFRP

$$V_f = \frac{37.659}{0.85} = 44.305 \text{ KN}$$

d) Shear force taken by CFRP strip

The shear contribution of the FRP can be than calculated from (ACI440.2R-17:11.4a)

$$V_{f(act.)} = \frac{d_f}{S_f} A_{fv} f_{fe} \quad \dots(3.8)$$

Where A_{fv} = The area of CFRP shear reinforcement

f_{fe} = The effective strain in the CFRP

$$V_{f(act.)} = \frac{d_f}{S_f} (2t_f b_f) E_f \varepsilon_{fe}$$

$$\text{So } \varepsilon_{fe} = K_v * \varepsilon_{CFRP} \quad \dots(3.9)$$

$$= K_v * \varepsilon_{CFRP} = \frac{K_1 K_2 l_e}{11900} \quad \dots(3.10)$$

Coefficient of concrete strength

$$K_1 = \left(\frac{f'_c}{27}\right)^{2/3} \quad \dots (3.11)$$

$$= \left(\frac{30}{27}\right)^{2/3}$$

$$= 1.0728$$

Active bond length

$$\begin{aligned} L_e &= \frac{23300}{(n \cdot t_f \cdot E_f)^{0.58}} \quad \dots (3.12) \\ &= \frac{23300}{(1.2 \cdot 165000)^{0.58}} \\ &= 19.737 \text{ mm} \end{aligned}$$

Coefficient for type of wrapping scheme used

$$\begin{aligned} K_2 &= \frac{d - 2L_e}{d} \quad \text{For 2-side bond.} \quad \dots (3.13) \\ &= \frac{300 - 2 \cdot 19.737}{300} \\ &= 0.86842 \end{aligned}$$

So effective strain in CFRP

$$\begin{aligned} \varepsilon_{fe} &= K_v \cdot \varepsilon_{CFRP} \quad \dots (3.14) \\ &= \frac{K_1 K_2 l_e}{11900} \\ &= \frac{1.0728 \cdot 0.86842 \cdot 19.737}{11900} \\ &= 0.0015452 \leq 0.004 \text{ (ACI440.2R-17:11.4.1.2e)} \end{aligned}$$

The effective strain in the FRP shear strengthening system is limited in ACI440.2R-17 to prevent detachment failures and also maintain the interlock of the concrete member. So above condition is satisfied, bond strain have been analysed to determine the efficiency of these system and effective strain that can be achieved.

$$\begin{aligned} \text{So } V_{f(\text{act.})} &= \frac{300}{100} (2 \cdot 1.2 \cdot 50) \cdot 165000 \cdot 0.0015452 \\ &= 91.784 \text{ KN} > 44.305 \text{ KN } (V_f) \end{aligned}$$

3.7 Total shear calculation

$$\begin{aligned} \text{Total force } \frac{P}{2} &= 46.05 + 91.784 \\ &= 137.8344 \text{ KN} \\ \mathbf{P} &= \mathbf{275 \text{ KN}} \end{aligned}$$

The above analytic calculation shows the ultimate shear strength of CFRP strengthen RC beam to be 275 KN. That is closure to experimental results (270 KN).

Chapter-4

Numerical Solution for RC beam

In this chapter the FEM model in ABAQUS, material behaviour, loading condition, boundary condition, Element type and mesh convergence study have been discussed. Here a quarter model of the beam is built to save simulation time. Here different results have been shown by making changes such FRP part shell and solid, FRP layer single, composite and cohesive layer by creating offset. After all parametric study, results are compared to experimental data.

4.1 Shear Test Specimen used for experiment

Test specimen used for modelling, is same as model used in the paper published by **Obaidat et al. (2010)**. In this paper experimental works for Flexure and shear strengthening in different group like RF/RS are done.

We have selected to work on RS group for shear strengthening. The beam cross-section was 150×300mm and length- 1960 mm. To study shear behaviour, beam was ensured to fail in shear before flexure. So, less shear reinforcement and more tension reinforcement are casted. Here induced tension side reinforcement (2 Φ 18), compression side reinforcement (2 Φ 10) and shear stirrups of 8 mm with centre to centre spacing is 400 mm as shown in Fig. 4.1 and centre to centre span length is 1560 mm. In all beams concrete cover of 25mm was provided to the main tension reinforcement.

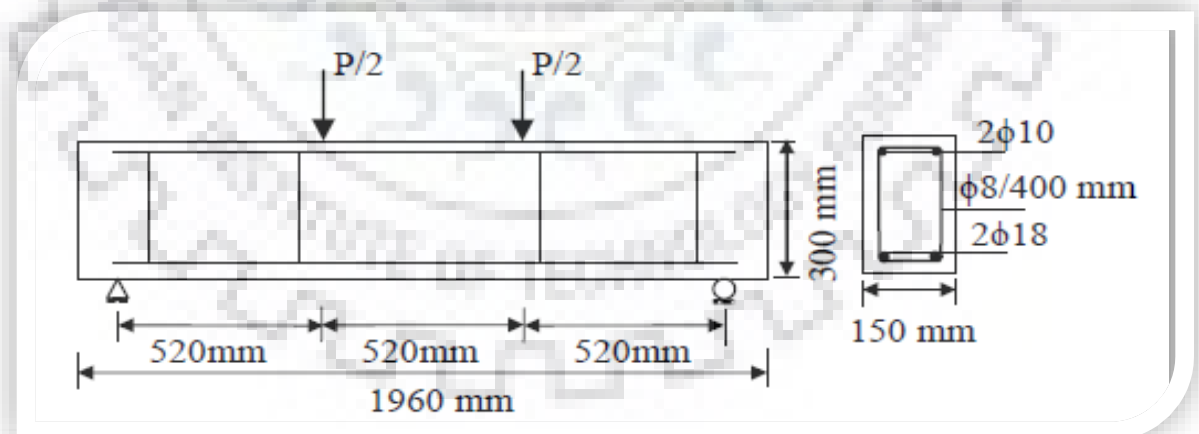


Fig. 4.1 Geometry and reinforcement of beam.

Four-point bending test was used in this experiment. The load was applied at points dividing the length into three equal parts of beam. To measure deflection of beam at mid-span LVDT is utilized as shown in Fig. 4.2.

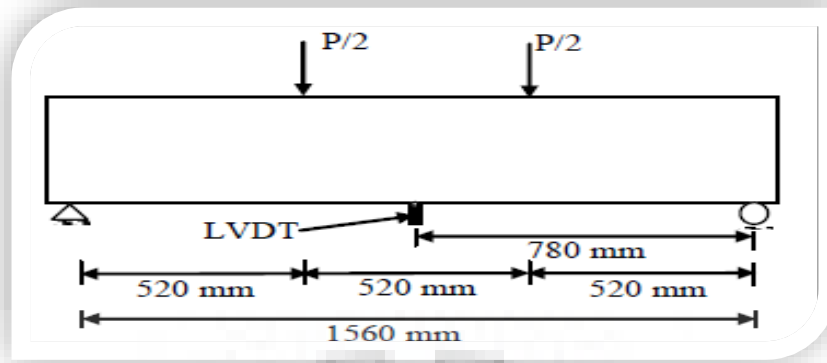


Fig. 4.2 Loading, supports and LVDT's position

For group RS, CFRP sheets which was 50 mm wide and 300 mm long are used to retrofit the beam web on both the faces as shown in Fig. 4.3. Epoxy adhesive was used for bonding of CFRP laminate to concrete, which has 1mm thin and 40 MPa compressive strength.

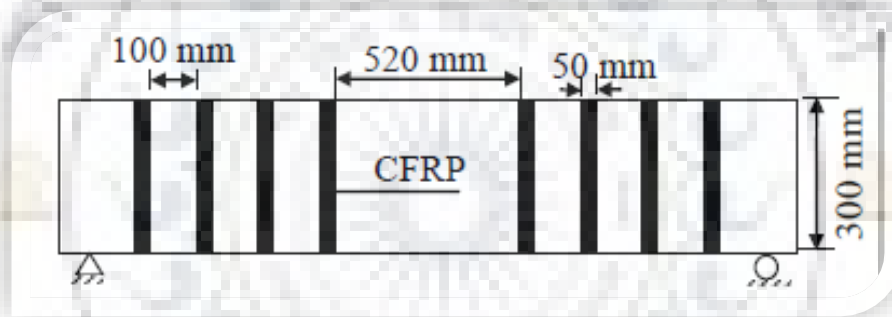


Figure 4.3 Arrangement of CFRP laminate in retrofitted beams.

Following mechanical properties of materials are used in experimental works given Table 4.1

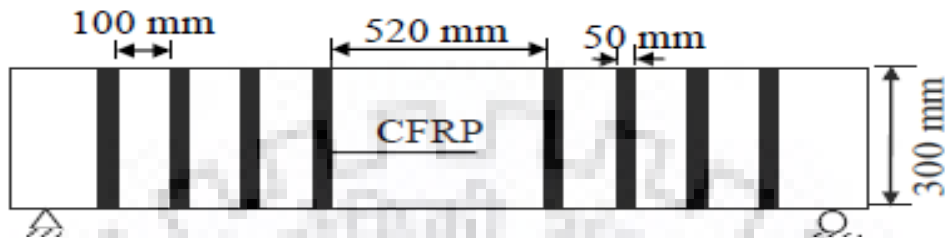
Table 4.1 Mechanical properties of materials used.

Materials	Notation	Properties
Steel	f_y	507 MPa
	E_s	210 MPa
	ν	0.3
Concrete	f'_c	30 MPa
CFRP	E_f	165 GPa
	f_f	2 GPa

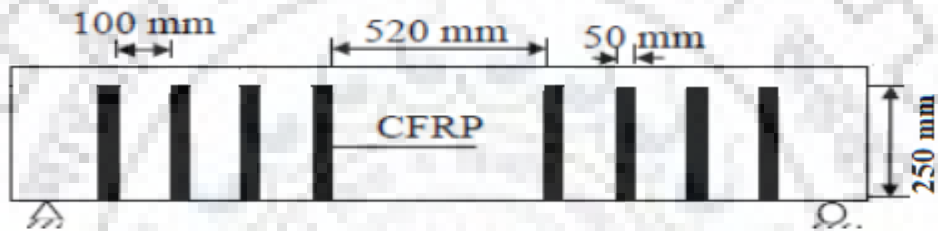
4.2 Numerical model and materials properties

4.2.1 Beam models studied

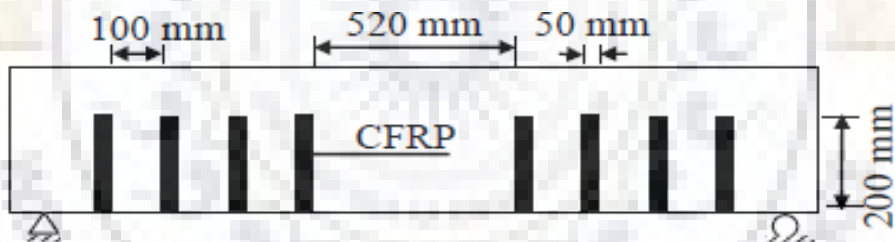
In order to study how length and orientation of FRP affect the shear behaviour of strengthening beam, numerical simulations were conducted in five steps of length and 90° and 45° orientations with respect to beam axis shown in Fig. 4.4 and experimental results are validated.



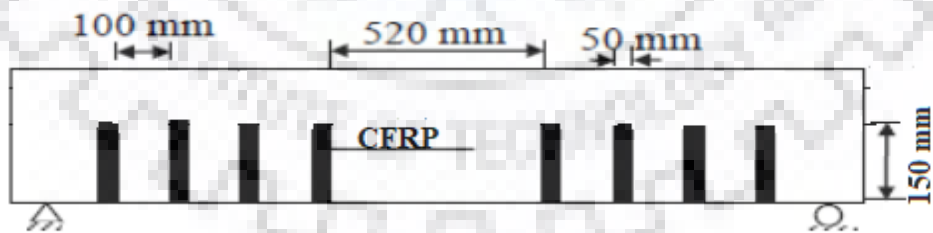
(a) RB 90/300



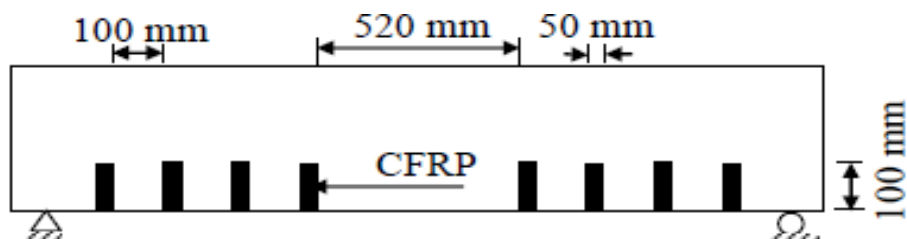
(b) RB 90/250



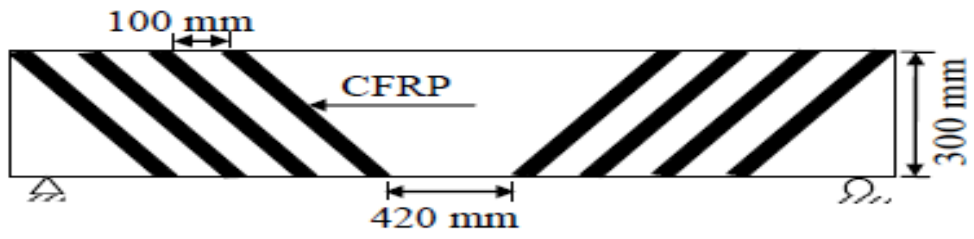
(c) RB 90/200



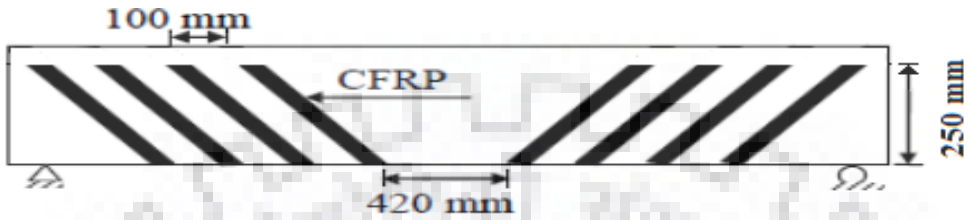
(d) RB 90/150



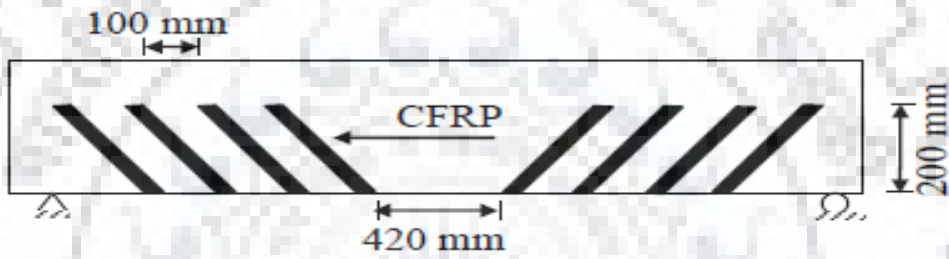
(e) RB 90/100



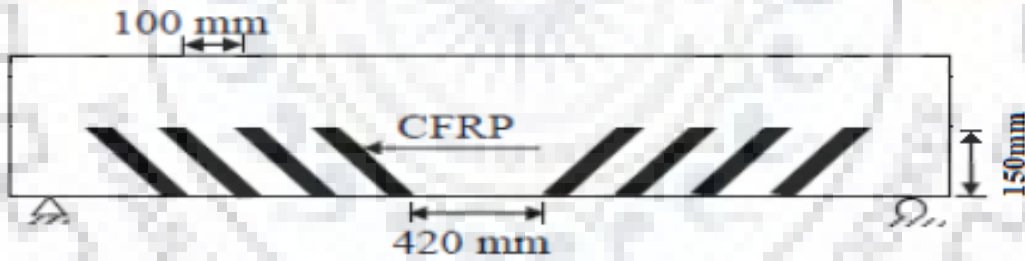
(f) RB 45/300



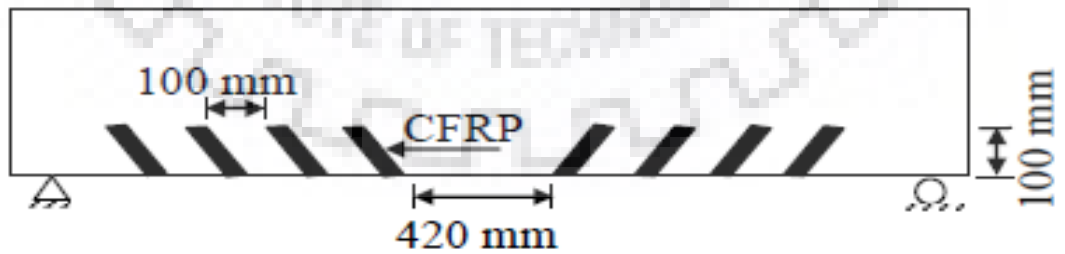
(g) RB 45/250



(h) RB 45/200



(i) RB 45/150



(j) RB 45/100

Fig. 4.4 Experimental setup

4.2.2 Material models

4.2.2.1 Concrete

Here concrete properties were taken from **Obaidat et al. (2010)**. There are several concrete crack models - discrete crack model, concrete damaged plasticity model and smeared crack model. All three-type of crack model provides a general capability for modelling concrete in all types of structure such as beams, trusses, shells, and solids.

Smeared crack model and CDP model are useful for modelling plain concrete and reinforced structure. But cracking model useful for ceramics or brittle rocks. Smeared crack model is designed for applications where monotonic strain at low confining pressures is applied to concrete. But in CDP model, monotonic, cyclic, and dynamic loading is applied to concrete under low confining pressures.

When the discrete crack model is applicable in FEA. The crack is defined along boundaries, but overcoming computational difficulties due to re-meshing remains a challenge. The Smeared crack model is divided into two parts: the fixed smeared crack model and the rotating smeared crack model. The smeared failure analysis has been improved considerably by rotating crack and multi crack concept.

Drawback of the smeared crack model is called a phenomena of “**strain localization**”, lead to zero energy consumption during crack propagation as the element size approaches to zero. CDP model was utilized to study the behaviour of reinforced concrete as it can capture the behaviour of concrete in both compression and tension.

Here the plastic damage model is used. Compression or tensile crack are two modes of failure process of concrete. For defining concrete behaviour CDP properties has been used and it requires values of density, Elastic modulus $\{E_c\}$, Poisson ratio $\{\mu\}$, plastic parameters and tension and compression behaviour of concrete.

Also, some plasticity parameters such as **Dilation angle $\{\psi\} - 37^\circ$, Flow potential Eccentricity – 0.1** and some default value taken by ABAQUS $\frac{f_{b0}}{f_{c0}} = 1.16$, **K=0.666** are used and viscosity parameter does not affect analysis part but affect convergence part. Dilution angle $\{\psi\}$ lesser values define brittle behaviour and higher values define ductile behaviour.

For concrete under uniaxial compression, **Saenz’s stress-strain relationship** is adopted. Compressive stress behaviour is defined in tabular form as yield stress vs inelastic stain. Inelastic strain is defined as total strain minus elastic strain.

$$\sigma = \frac{\alpha \varepsilon}{1 + \left[\left(\alpha \frac{\varepsilon_p}{\sigma_p} \right) - 2 \right] \left(\frac{\varepsilon}{\varepsilon_p} \right) + \left(\frac{\varepsilon}{\varepsilon_p} \right)^2} \quad \dots (4.1)$$

In above equation σ and ε are denotes the compressive stress and strain respectively, σ_p and ε_p are the experimentally determined maximum compressive stress and the corresponding strain, and the coefficient α is an experimentally determined the initial tangent modulus. In this analysis α was taken equal to Elastic modulus of concrete (E_c), σ_p taken equal to cylinder compressive strength of concrete and ε_p equal to 0.002 respectively. Graphical representation of nonlinear compressive behaviour of concrete is shown in Fig. 4.5. Hence some elastic parameter is calculated according to **ACI-318 code**.

Cylinder compressive strength $f'_c = 30$ MPa.

Elastic modulus $E_c = 4700\sqrt{f'_c} = 26,000$ MPa ...(4.2)

Tensile strength $f_{ct} = 0.33\sqrt{f'_c} = 1.81$ MPa ...(4.3)

Strain at maximum stress $\varepsilon_p = 0.002$

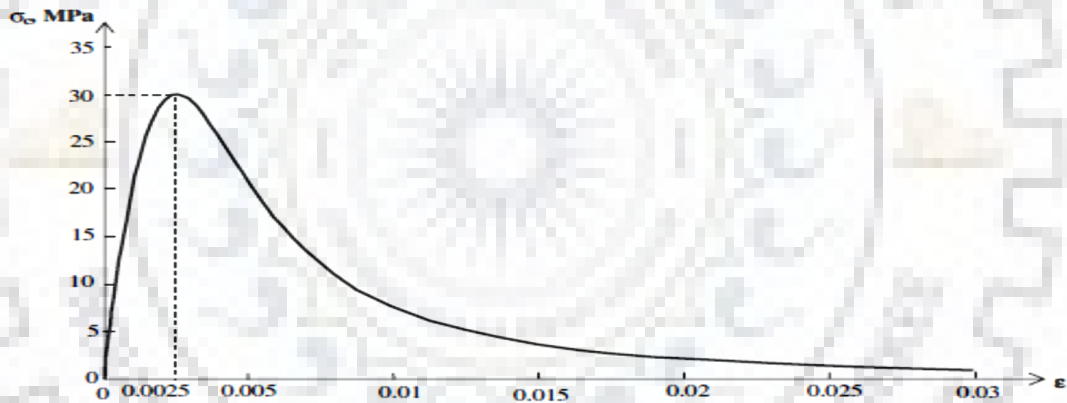


Fig. 4.5 Stress strain behaviour of concrete under uniaxial compression.

For concrete under uniaxial tension the stress and strain curve follow linear elastic behaviour as shown in Fig. 4.6(a) until failure strain is reached and failure stress corresponding to micro cracking on the concrete surface. Beyond failure stress formation of micro crack represents softening behaviour of concrete. Tension-softening curve proposed by **Hordijk** which was derived from an extension series of tensile test of concrete was used:

$$\frac{\sigma_t}{f_t} = \left[1 + \left(c_1 \frac{w_t}{w_{cr}} \right)^3 \right] e^{\left(-c_2 \frac{w_t}{w_{cr}} \right)} - \frac{w_t}{w_{cr}} (1 + (c_1)^3) e^{(-c_2)} \quad \dots (4.4)$$

Where crack opening displacement at the complete release of stress or fracture energy is reached

$$w_{cr} = 5.14 \frac{G_F}{f_t} \quad \dots (4.5)$$

Here w_t is the crack opening displacement.

w_{cr} is a crack opening displacement at full stress release of concrete or G_F complete released.

σ_t is the tensile stress normal to the crack direction.

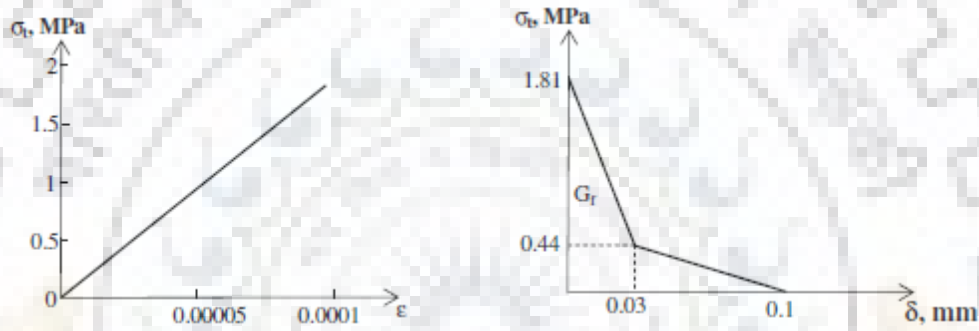
f_t is the concrete tensile strength under uniaxial tension,

G_F is the fracture energy required to create a stress-free crack over a unit area.

$c_1=3.0$ and $c_2=6.93$ are constants determined from tensile tests of concrete.

G_F is area under tensile softening curve of concrete shown in Fig 4.6(b) assume 90 J/m^2 .

Tensile strength of concrete is $f_{ct} = 0.35\sqrt{f'_c} = 1.81 \text{ MPa}$... (4.6)



(a) Stress-strain relationship up to ultimate load. (b) Post-peak stress deformation relationship.

Fig. 4.6 Concrete under uniaxial tension.

4.2.2.2 Steel

Here steel is assumed elastic and perfectly plastic material with stress-strain relationship shown in Fig. 4.7. These are some Experimental values of steel reinforcement used in FEM model.

Elastic modulus of steel reinforcement $\{E_s\} = 209\text{MPa}$,

Yield stress of steel reinforcement $\{f_y\} = 507\text{MPa}$

Poisson ratio $\mu=0.3$

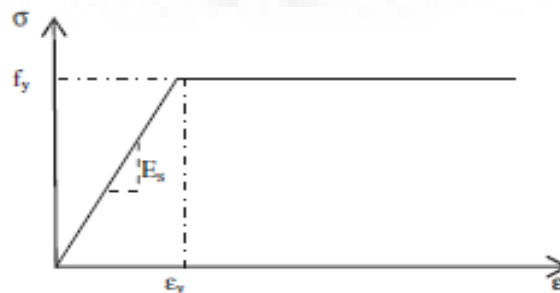


Fig. 4.7 Stress strain behaviour of steel

Plastic behaviour of steel is defined in terms of yield stress of 507MPa and corresponding plastic strain is taken zero in ABAQUS. Interactions between steel and concrete are perfect bond. Host region was taken as concrete whereas embedded region was selected to be reinforcement. Model reinforcement is shown in Fig. 4.8.

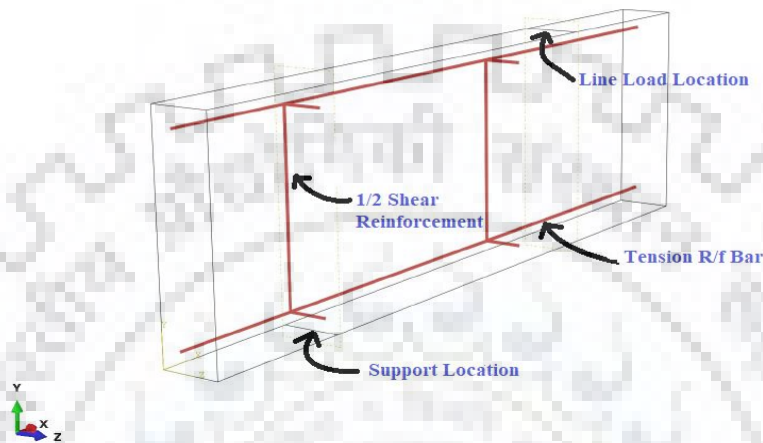


Fig. 4.8 Model of concrete beam with reinforcement

4.2.2.3 FRP material

FRP is composite material of fibres and resin such as epoxy. Where reinforcing fibres such as carbon, glass, basalt and aramid provide strength and stiffness and matrix protects fibres from damaged caused by abrasion and impact and helps in spreads the load and arrange the fibres in particular orientation. FRP composite provide high strengths and stiffness, easy to moulding complex shapes, high environmental resistance, all coupled with low densities, make the resultant composite superior to metals and many applications.

Here two types of model are considered - liner elastic isotropic until failure and liner elastic orthotropic material. If fibres are aligned in one direction and it is known as unidirectional.

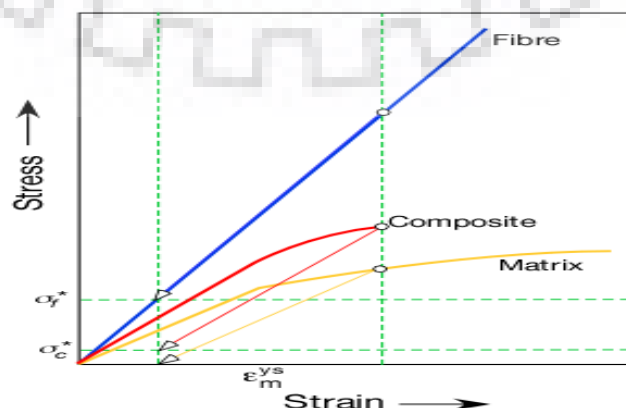


Fig. 4.9 Elastic brittle fibre & Elastic-plastic Matrix

In composite material tensile behaviour is shown in Fig. 4.9. If composite further increase in load-deflection then the matrix will be deforming plastically, while embedded fibre continues to stretch elastically and in composite stress-strain increase in non-linear fashion. Unloading behaviour of fibre is shown in figure above.

The overall mechanical behaviour of composites is determined by:

1. The properties of the fibres
2. The properties of the resin
3. The ratio of fibre to resin in the composite (volume fraction)
4. The orientation and geometry of the fibres in the composite.

Orthotropic behaviour of composite is assumed engineering constants induced in FEM software. Properties of fibres used for analysis in model are shown in Table 4.2. Here volume fraction of fibres is taken as 75 % in all cases so engineering constants. All fibres are found using Rule of Mixture and Inverse Rule of Mixture as given below

Young Modulus:

$$E_{11} = V_f E_f + V_m E_m \quad \dots (4.7)$$

$$\frac{1}{E_{22}} = \frac{V_f}{E_f} + \frac{V_m}{E_m} \quad \dots (4.8)$$

$$E_{33} = E_{22} \quad \dots (4.9)$$

Shear Modulus:

$$\frac{1}{G_{12}} = \frac{V_f}{G_f} + \frac{V_m}{G_m} \quad \dots (4.10)$$

$$G_{13} = G_{12} \quad \dots (4.11)$$

Poisson's Ratios:

$$\nu_{12} = V_f \nu_f + V_m \nu_m \quad \dots (4.12)$$

$$\nu_{13} = \nu_{12} \quad \dots (4.13)$$

Table: - 4.2 Mechanical properties of FRP

Material	E_{11} (GPa)	E_{22} (GPa)	E_{33} (GPa)	G_{12} (GPa)	G_{13} (GPa)	G_{23} (GPa)	ν_{12}	ν_{13}	ν_{23}
Carbon	165	9.65	9.65	5.2	5.2	3.4	0.3	0.3	0.45
Basalt	70.375	9.253	9.253	4.988	4.988	3.261	0.28	0.28	0.431
E- Glass	56.125	9.07	9.07	4.906	4.906	3.207	0.265	0.265	0.425

4.2.3 Modelling of FRP-concrete interface

For interface between concrete and FRP two different models are used – one is perfect bonding another is cohesive bonding. Cohesive bonding is defined using simple bilinear traction separation law shown in Fig. 4.10. It follows linear elastic until damage initiation followed by evolution of damage, in which elements start to degrade. Graphical representation in terms of effective traction τ and effective opening displacement δ is shown below.

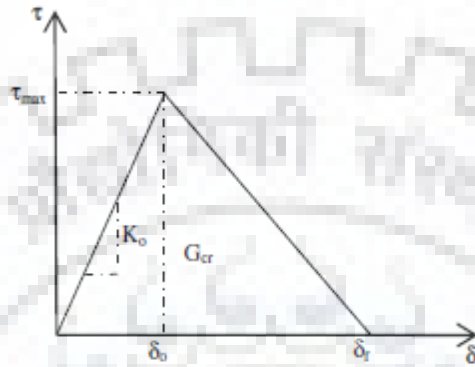


Fig. 4.10 Bilinear traction–separation constitutive law.

Initial stiffness K_0 is

$$K_0 = \frac{1}{\frac{t_i}{G_i} + \frac{t_c}{G_c}}$$

Where, Thickness of resin $\{ t_i \} = 1\text{mm}$,

Thickness of concrete $\{ t_c \} = 5\text{mm}$,

Shear modulus of resin $\{ G_i \} = 0.665\text{ GPa}$

Shear modulus of concrete $\{ G_c \} = 10.8\text{ GPa}$.

According to Fig. 4.10 traction stress depend on initial stiffness K_0 and energy required for crack opening $\{ G_{cr} \}$ is area under the curve. τ_{max} is a maximum stress and δ_f is a crack opening displacement of fracture.

Initiation of damage is assumed to occur when following quadratic traction function sum of the

following stress ratios become one. Representation follow in given eq.

$$\left\{ \frac{\sigma_n}{\sigma_n^0} \right\}^2 + \left\{ \frac{\tau_n}{\tau_n^0} \right\}^2 + \left\{ \frac{\tau_t}{\tau_t^0} \right\}^2 = 1$$

Where, σ_n is cohesive tensile stress of interface. τ_n and τ_t are cohesive shear strengths of the interface.

$$\sigma_n^0 = f_{ct} = 1.81 \text{ MPa}, \sigma_s^0 = \tau_t^0 = 1.5 \text{ MPa are used.}$$

Damage evolution is defined in terms of fracture energy based on the Benzaggah-Kanane fracture criteria. Value used for study in ABAQUS is $G_n^c = 90 \text{ J/m}^2$, $G_t^c = G_s^c = 900 \frac{\text{J}}{\text{m}^2}$ and $n = 1.45$.

4.3 Meshing and Modelling

Here four node linear tetrahedral elements for concrete and FRP plate (solid) are used and reinforcement of steel is in wire form, therefore no need of any element type for meshing of RC wire. This element has four nodes with 3-degree of freedom at each node-translation in the x, y, and z directions. C3D4 Element configuration is shown in Fig. 4.11

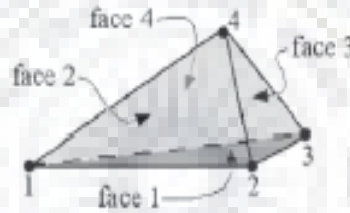


Fig. 4.11 4-Node linear tetrahedral element.

In general, all triangular and tetrahedral elements in Abaqus use to full integration. Quadrilateral and hexahedral elements can be used to reduced integration. The reduced integration elements have following advantage

- The first advantage is that strain and stress are calculated at the location that provide optimal accuracy.
- The second advantage is that the CPU time and storage requirement decrease.

The procedure can admit deformation modes that cause no straining at the integration points is disadvantage of reduced integration.

Generally, full integration elements are not suitable for the analysis of incompressible behavior of material. Because the material behavior forces the material to deform without volume changes. Fully integrated element meshes, and in particular lower-order element meshes, do not allow deformations (other than purely homogeneous deformation). Because

Abaqus uses “selectively reduced” integration in these elements: reduced integration is used for the volume strain and full integration for the deviatoric strains.

In order to reduce analysis time, one quarter of beam was modelled as shown in Fig. 4.12, concrete beam is 3D solid type, tension and compression reinforcement or stirrup is 3D wire planar type. FRPs were created in two ways one is 3D solid another 3D shell. Here parametric study all of way of FRP in perfect bonding such as solid and shell tie, solid and shell composite tie and solid cohesive are analysed.

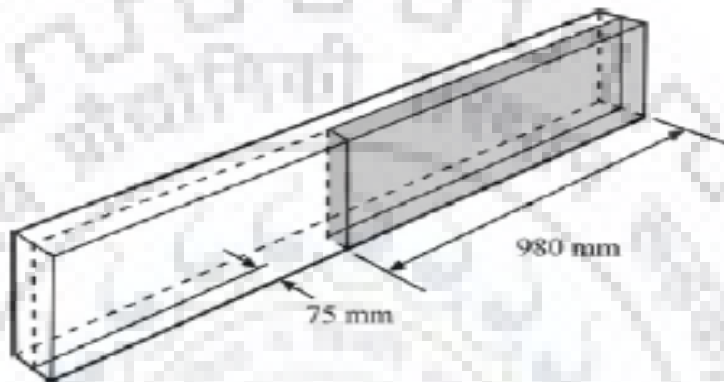


Fig. 4.12 One quarter of beam using symmetry

Properties are defined and assigned to every part. Reinforcement bar and stirrup are assigned beam section orientation also. Then in FRP first separate Datum plane of every FRP layer is created and assigned material orientation in fibre direction.

For boundary condition a set of lines are created at support and load location. Then initial boundary condition at supported hinge, after then Step 1 provide downward deflection at load location. Due to plane symmetry in XY-plane, Z-symmetry is provided and in YZ-plane, X-symmetry is provided as shown in Fig. 4.13 and 4.14.

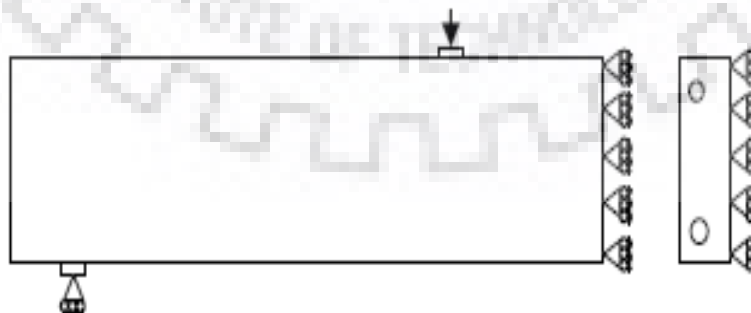


Fig. 4.13 Boundary conditions

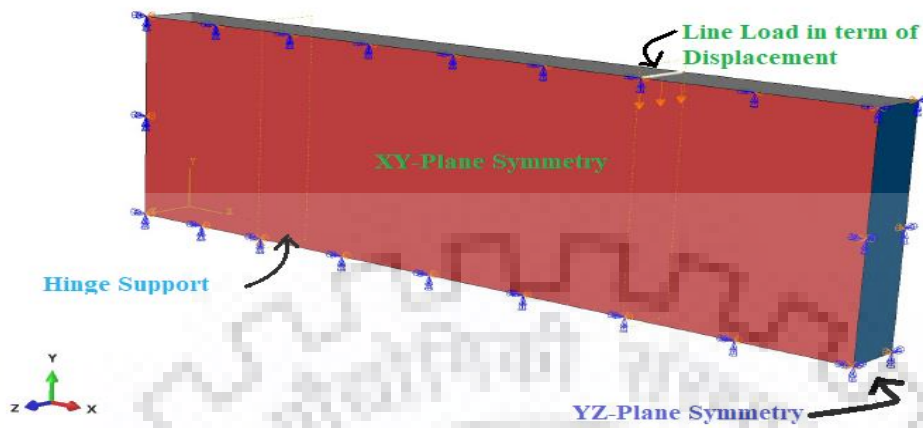


Fig. 4.14 Model boundary condition.

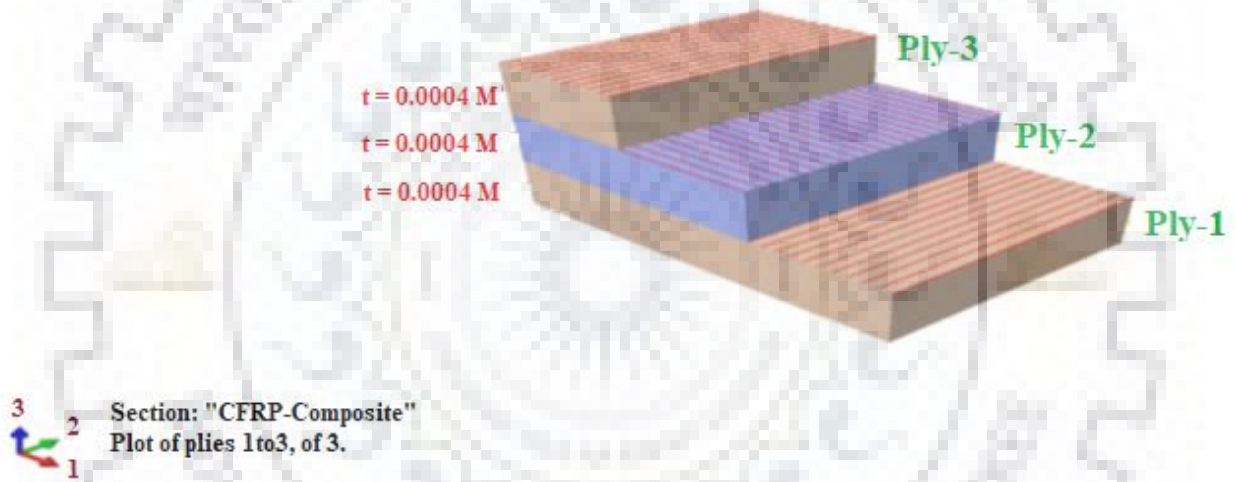


Fig. 4.15 Orientation of fibres in each composite layup

Finite analysis mesh of beam is bilinear tetrahedral as shown in Fig. 4.16.

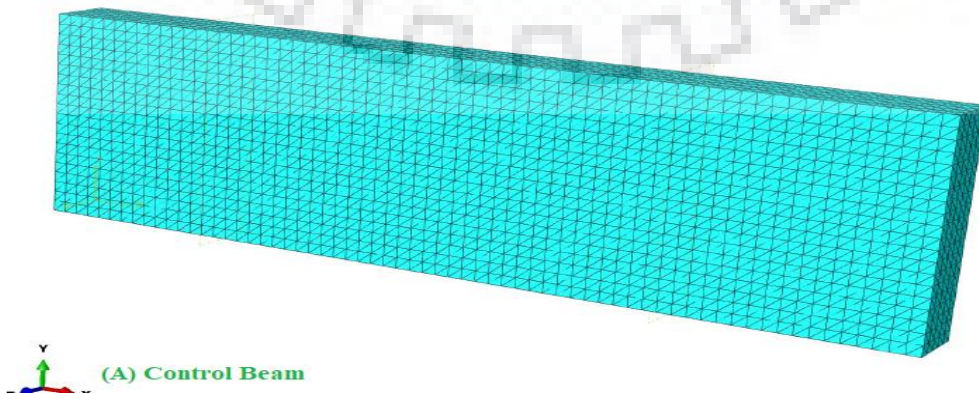




Fig. 4.16. Finite element mesh of a quarter of control & strengthened beam

In Table 4.3 shows that number of elements, number of nodes, number of variable (degree of freedom plus maximum number of Lagrange multiplier variable) and CPU time in term of second.

Table 4.3 Number of elements, nodes, variable and CPU time of Different Models.

S No	Model	Number of elements	Number of nodes	Number of variable (DOF + max. no of any Lagrange multiplier variable)	Job time (CPU time) (sec)
1.	Control beam	41348	62405	186699	55413
Strengthened beam					
2.	Perfect single layer	42810	65857	197055	74961
3.	Perfect composite layer	43722	67717	202635	56576
4.	Cohesive model	43290	66193	198063	51917
Types of FRP					
5.	CFRP-250	45715	69755	208551	50111
6.	CFRP-200	44518	67678	202518	50529

7.	CFRP-150	44946	68055	203649	55503
8.	CFRP-100	45590	68762	205770	58068
9.	BFRP-300	42810	65857	197055	56248
10.	BFRP-200	44518	67678	202518	55314
11.	BFRP-100	45590	68762	205770	50107
12.	E-GFRP-300	43722	67717	202635	51774
13.	E-GFRP-200	44518	67678	202518	52310
14.	E-GFRP-100	45590	68762	205770	56083
CFRP 45° Orientation					
15.	CFRP-300	53576	81862	244272	85032
16.	CFRP-250	49126	74878	224118	58839
17.	CFRP-200	47670	72533	217083	55583
18.	CFRP-150	46746	70875	212109	52392
19.	CFRP-100	45469	68726	205662	34464
Percentage of steel					
20.	CONTROL-14	41348	62405	186699	321390
21.	CONTROL -16	41348	62405	186699	86798
22.	CONTROL -18	41348	62405	186699	55413
23.	CONTROL -20	41348	62405	186699	37228
24.	CONTROL -25	41348	62405	186699	37428
25.	CONTROL -32	41348	62405	186699	40508
26.	CFRP-14	42810	65857	197055	61381
27.	CFRP-16	42810	65857	197055	45423
28.	CFRP-18	42810	65857	197055	74961
29.	CFRP-20	42810	65857	197055	46868
30.	CFRP-25	42810	65857	197055	49872
31.	CFRP-32	42810	65857	197055	46824

5.1 Introduction

In this chapter, overall study was done in three sections, convergence study of FEM model and validation of FEM model with experimental results and analytic results. After that, parametric study has been done to show the effect of shear behavior on strengthened beam by changing the FRP types (such as CFRP, BFRP and E-GFRP) with respect to length. In addition, orientation of CFRP and effect of percentage of steel were also studied.

The results obtained have been compared in form of load and mid-span deflection curve, deflection behavior, strain and ultimate load to study effect of different parameters on beam. After then, it has been tried to understand which parameters have most considerable effect on beam. Therefore, finite element model has been used to estimate these effects.

5.2 Convergence study of FEM model

5.2.1 Control beam

In the control beam convergence study has been done with respect to different mesh size of reinforced concrete beam such as 30mm, 20mm, 15mm and 12mm. So, in order to solve convergence problem small increment sizes has been used in STEP part and automatic stabilization has been used by specifying dissipated energy fraction of 2×10^{-5} . It had seen that load is decreasing with reduced mesh size as shown in Table 5.1, and come closure to experimental results. Graphical variation is shown in Fig. 5.1 and Fig. 5.2

Table 5.1 Load and deflection values

MESH SIZE	LOAD (KN)	DEFLECTION (MM)
30	287.895	6.0969
20	263.4254	6.38405
15	230.5982	6.76094
12	227.65076	7.53266

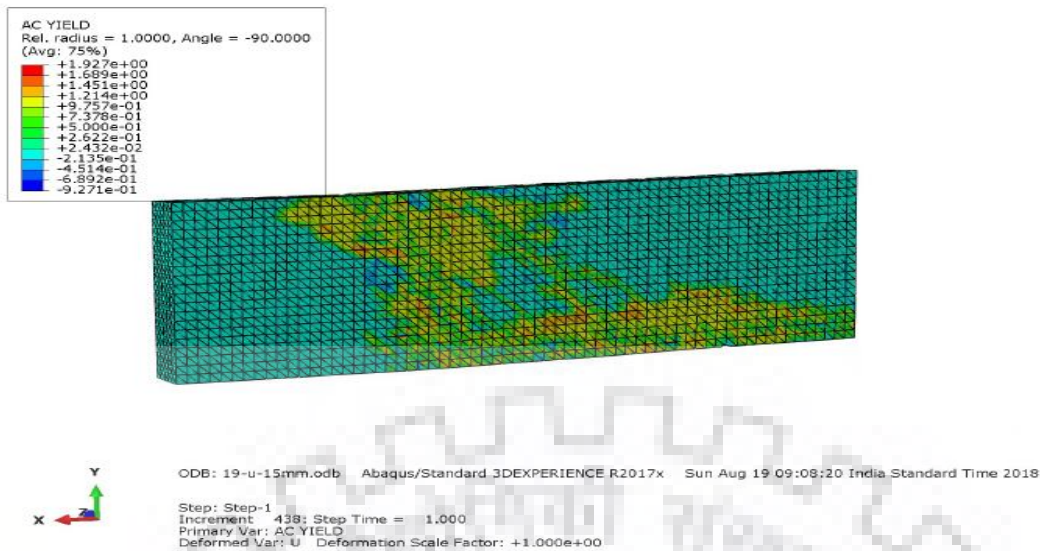


Fig. 5.1 Control beam yield behaviour in shear direction.

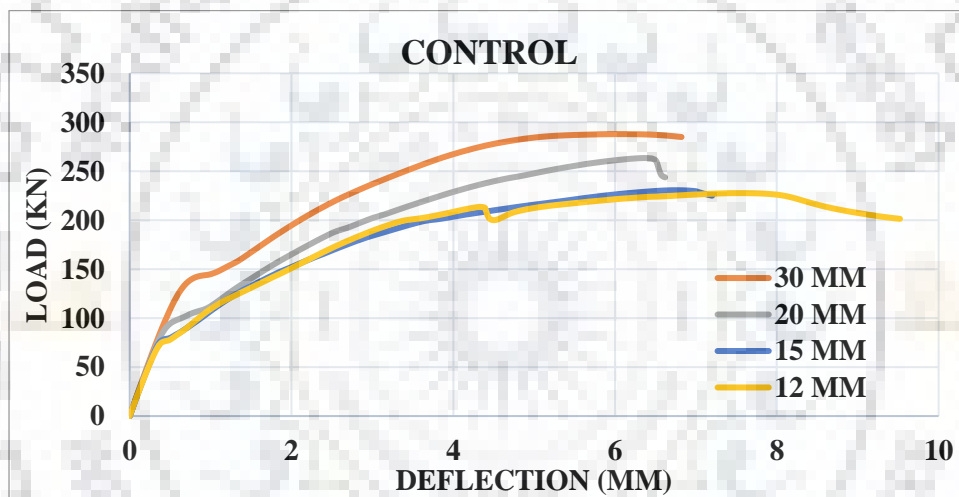


Fig. 5.2 Mesh convergence of control beam

5.2.2 Strengthened beam

In shear strengthening beam convergence study had been done with respect to FRP construction type, bonding between FRP and concrete surface, number of FRP layer such as single layer or composite layer and mesh size such as 30mm, 20mm and 15mm. In study of different mesh size reduction in the value mesh result is decreasing and come closure to experimental results. Load deflection value as shown in Table 5.2 and chart shown in Fig. 5.3.

Table 5.2 Load and deflection values for different Mesh

MESH SIZE	LOAD (KN)	DIFLECTION (MM)
30	296.5579	6.29182
20	263.0494	5.29839
15	262.3508	6.30268

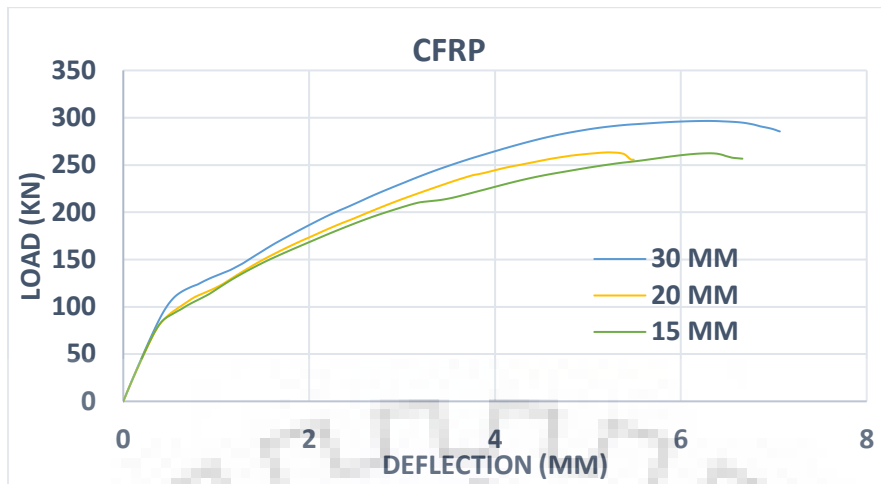


Fig. 5.3 Load vs deflection curve for different mesh size of strengthening beam

Table 5.3 shows results of different types of FRP construction load and deflection value for 15 mm mesh size. The cohesive model is created using zero mm cohesive offset layer concept. Graphical presentation has been shown in Fig. 5.4 and 5.5.

Table 5.3 Convergence of results of different FRP construction types

TYPE > BOND V	SOLID		SHELL	
	LOAD (KN)	DIFLECTION (MM)	LOAD (KN)	DIFLECTION (MM)
Perfect bonding				
SINGLE LAYER	262.3508	6.30268	259.1054	6.00129
COMPOSITE	256.6796	7.46954	267.9579	6.20217
Cohesive bonding	258.2692	6.29934		

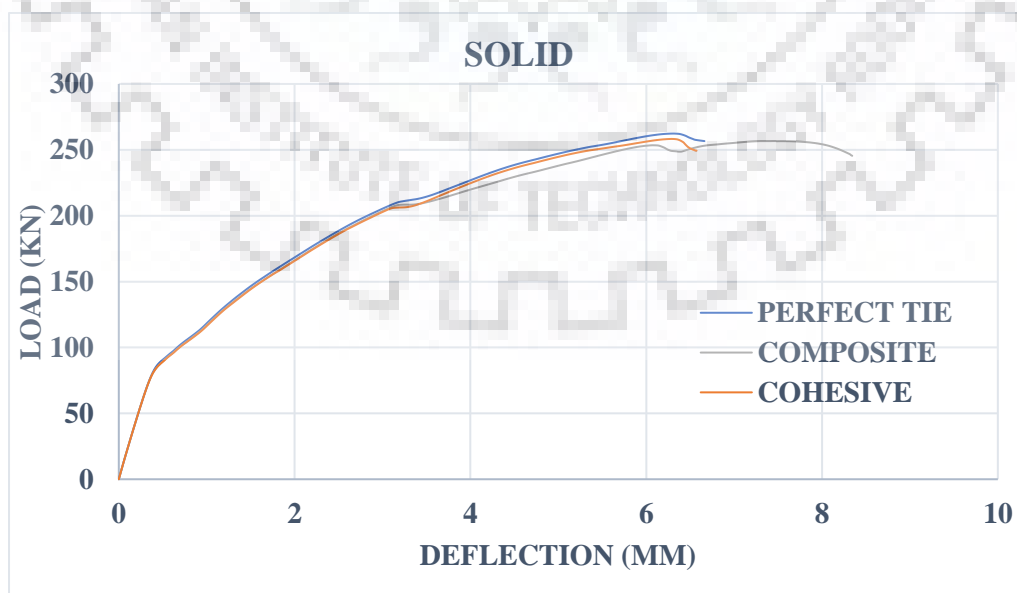


Fig. 5.4 Graphical result of solid layer of FRP

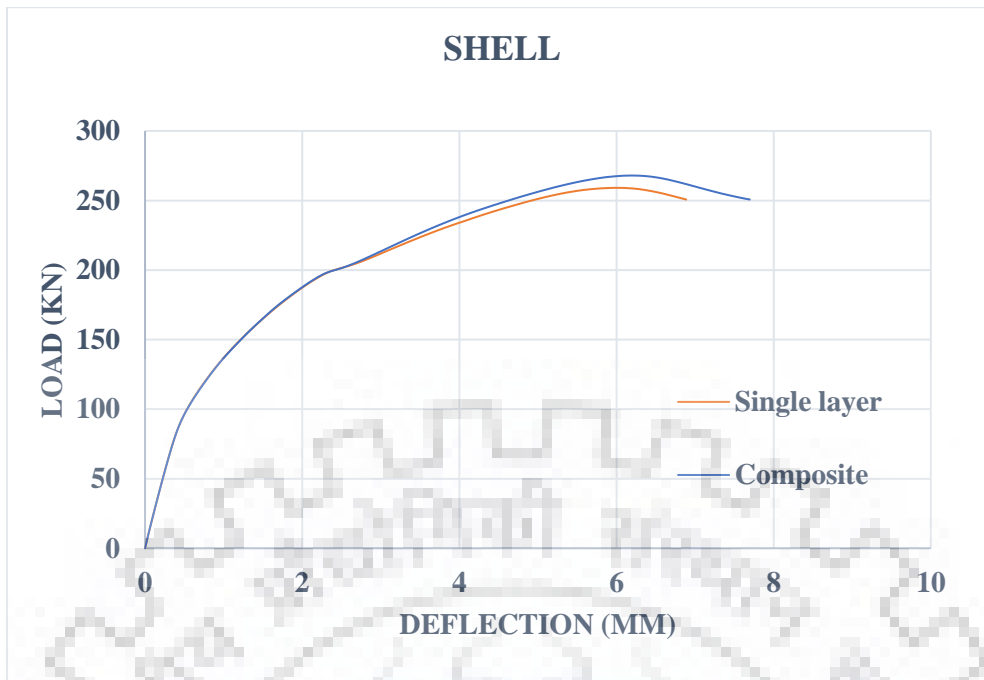


Fig. 5.5 Graphical result of shell layer of FRP

Yielding behaviour of concrete in strengthening beam in shear direction is shown in Fig. 5.6.

Printed using Abaqus/CAE on: Fri Apr 19 23:22:16 India Standard Time 2019

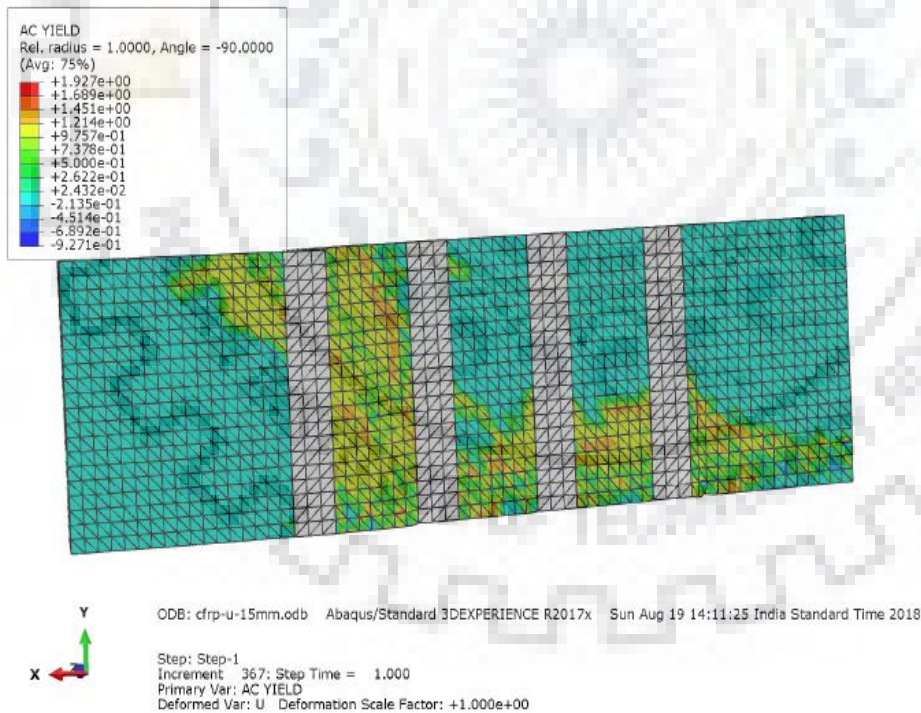


Fig. 5.6 Strengthened beam yield behaviour in shear direction

In whole convergences study 15 mm mesh size get accurate results. And all of construction and bonding of FRP get approximately equal results so here taken solid single layer FRP laminate for further study.

5.3 Validation of Results

In order to check accuracy of the results obtained from the FE model using ABAQUS have been verified with the results obtained from experimental studies (Obaidat 2007) and also verified with the FEM results developed in ABAQUS by Obaidat (2010). The mesh size, element types and all other properties of different components in the present model are same as considered by Obaidat (2010).

5.3.1 Control beam

Load–deflection curves for control beam present study compare with experimental and FEM results as shown in Fig. 5.7. In this comparison initial phase present beam shows more linear and take more load compare to experimental due to perfect bonding between concrete and steel in embedded region. Present beam fails after the experimental beam and equal to authentic published paper FEM result. As compare to experimental result our result was become **4% variation** in load and deflection values.

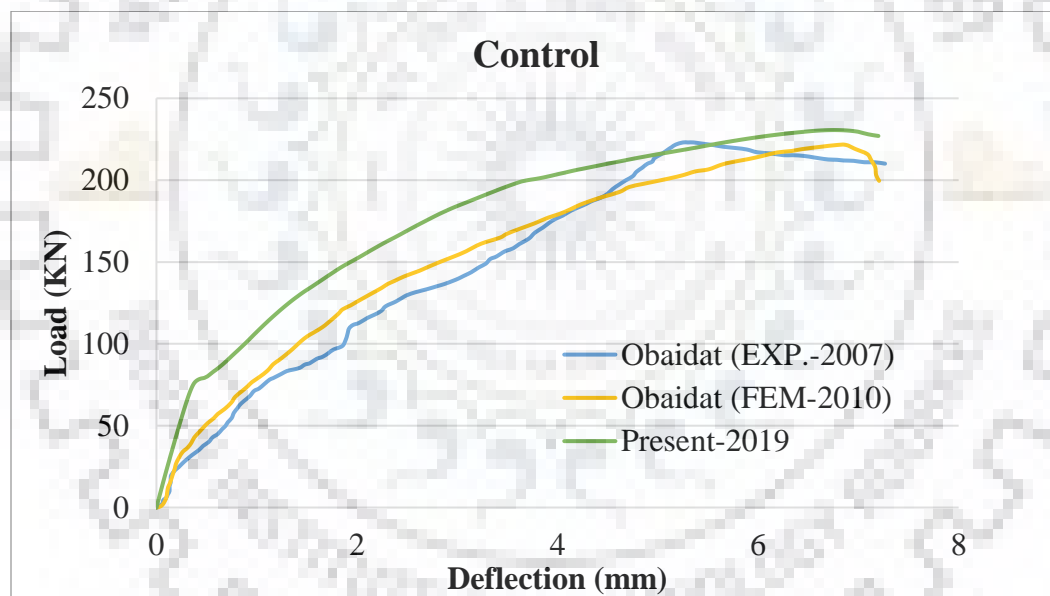


Fig. 5.7 Load vs Deflection curve of Control beam

5.3.2 Retrofitted Beam

In retrofitted beam load-deflection curve shown in Fig. 5.8. Here present failure load and experimental results become under **2.5%** variation (less) and author FEM model result (233.68 KN) was very less compare to Exp. and present model, due to some bonding mistake between FRP and concrete. In perfect bonding model fails to capture softening of the beam and therefore, unable to predict any debonding failure. Analytical results (**275 KN**) are close to experimental results. Fig. 5.10 and 5.11 show tension and compression damage of control beam while Fig.

5.12 and Fig. 5.13 show tension and compression damage of strengthening beam. Fig. 5.9 show downward deflection behaviour of quarter beam.

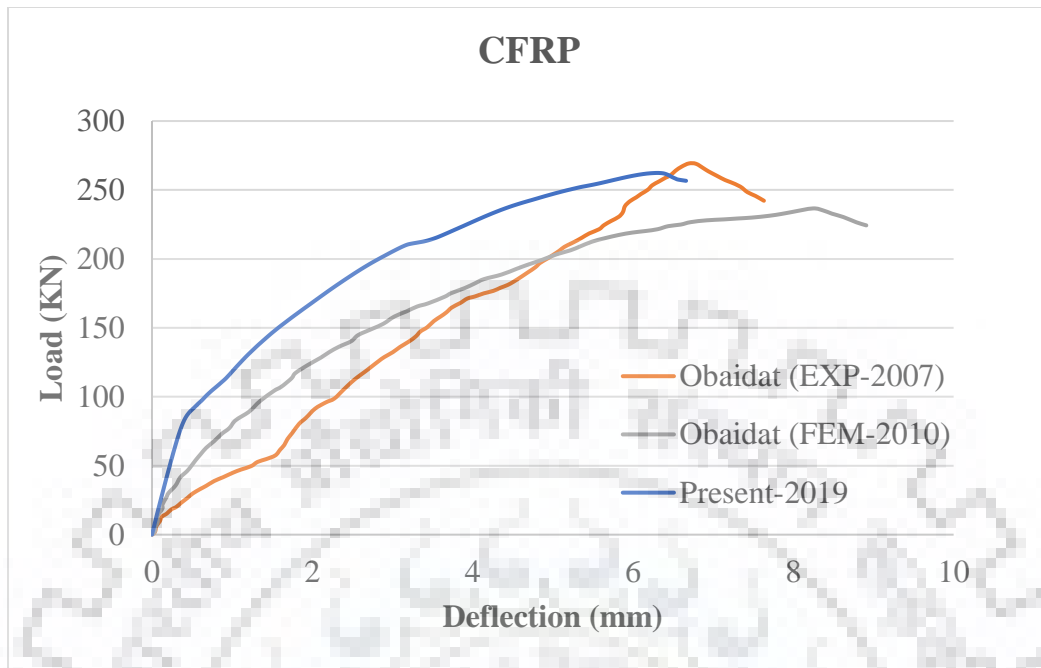


Fig. 5.8 Load vs Deflection curve of Retrofitted beam

Printed using Abaqus/CAE on: Fri Apr 19 23:22:55 India Standard Time 2019

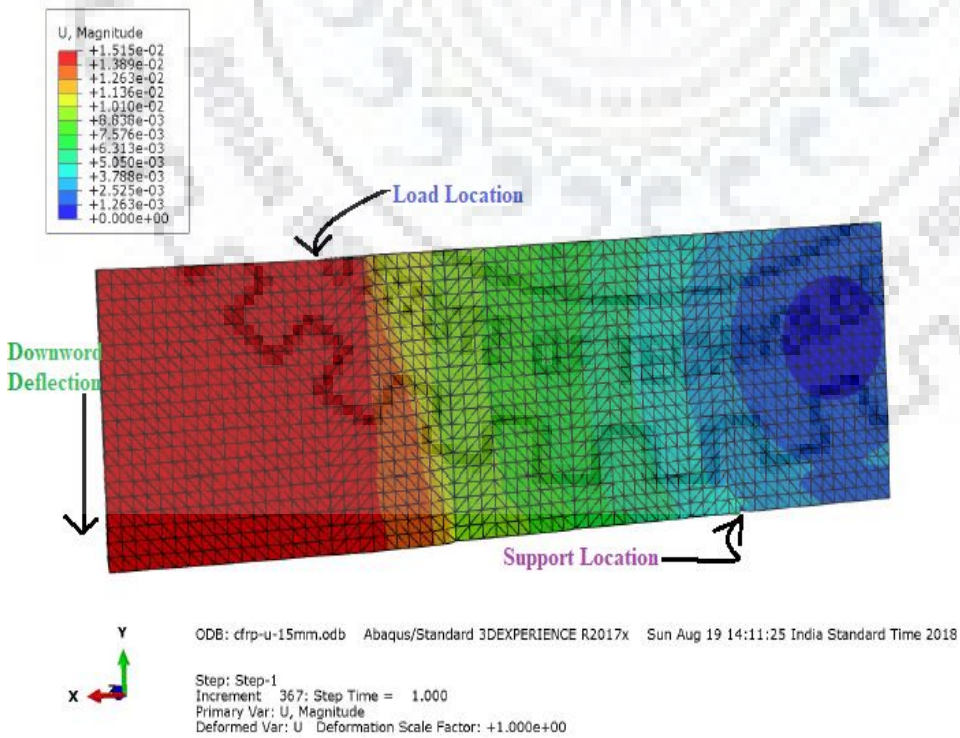


Fig. 5.9 Deflection of retrofitted Quarter beam

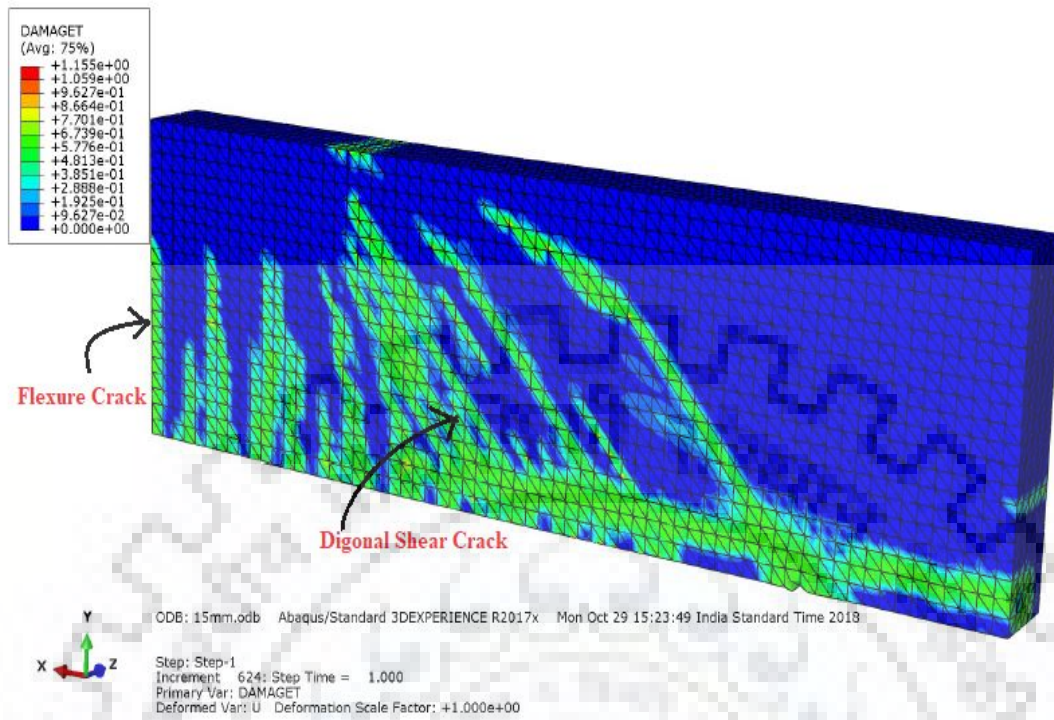


Fig. 5.10 tension damage control beam

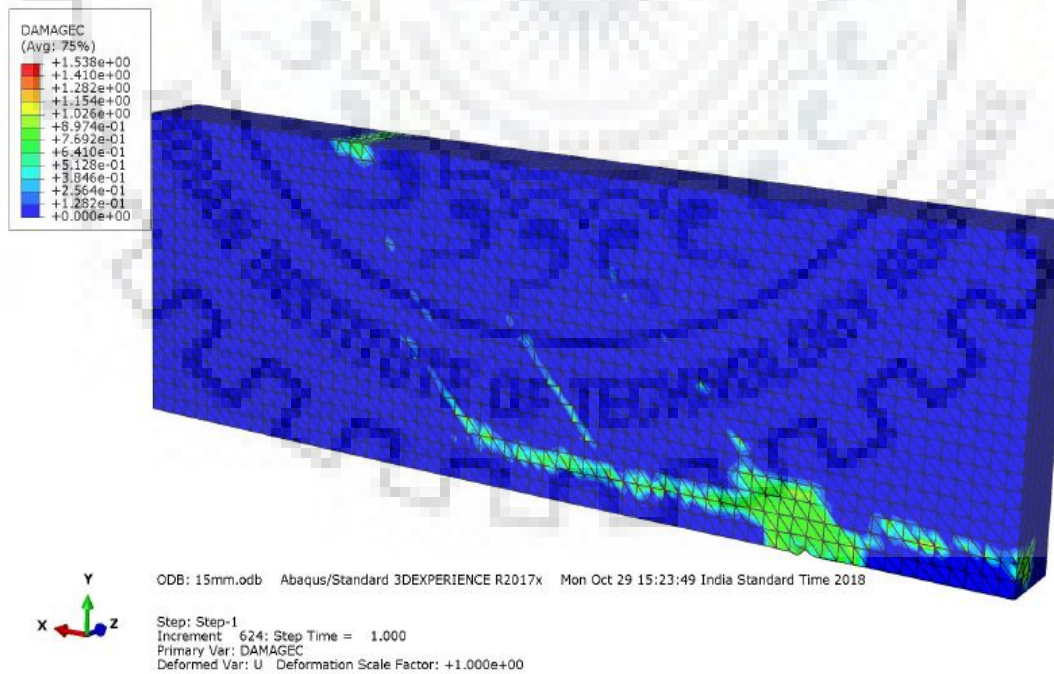


Fig. 5.11 compression damage control beam

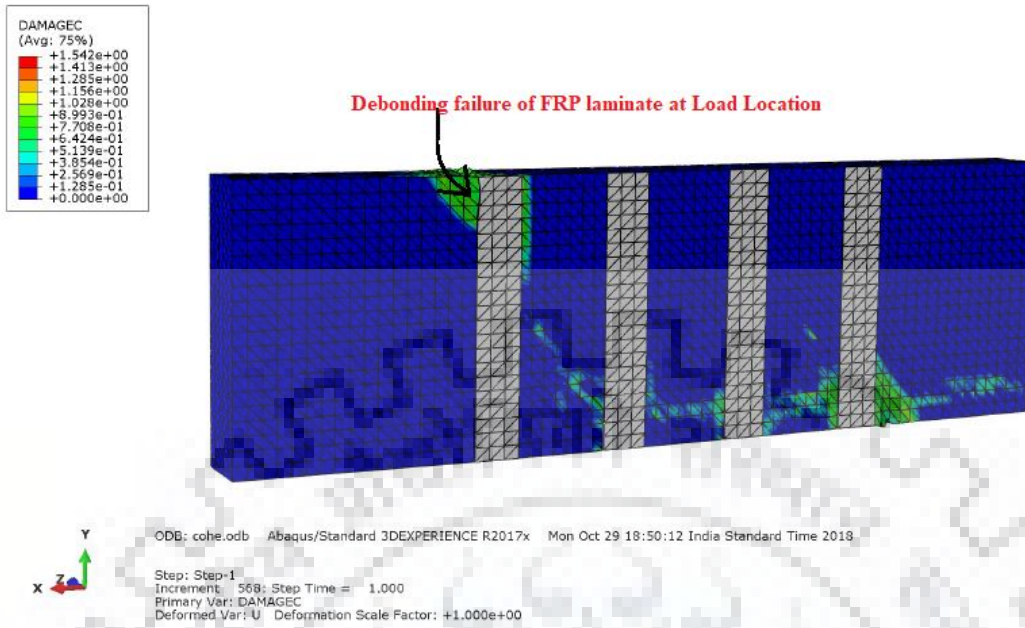


Fig. 5.12 Compression damage of strengthened beam

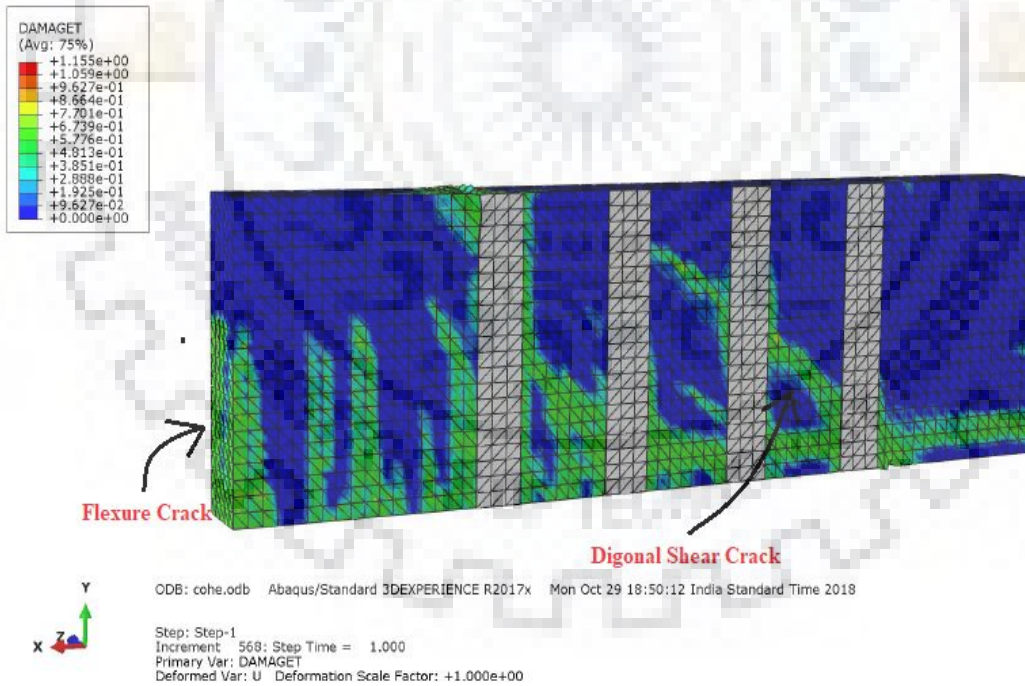


Fig. 5.13 Tension damage strengthened beam

In the above validated results, stiffness of the CFRP -strengthened beam was increased compared to control beams. The width of crack for strengthening beam was decrease as compared to control beam. In above cases initial part take higher stiffness and linear behaviour at pre loading stage then after stiffness is decreasing at the time of failure.

5.4 Parametric Study

5.4.1 Effect of different types of FRP's with respect to different heights

In this section, FRPs having different heights and materials are chosen for the study. Results obtained for different FRPs are given below in Table 5.4-5.5. Compared in variation of load and deflection are also shown Figs 5.14-5.16 for different height of FRP layers.

Table 5.4 Load vs deflection data of CFRP

S No.	Height (mm)	Deflection (mm)	Load (KN)	Percentage Variation	Secant Stiffness (KN/mm)
1.	300	6.30268	262.3508	2.021715	41.63
2.	250	6.67515	257.15192	3.355552	38.524
3.	200	7.36457	248.8032	4.410393	33.785
4.	150	6.80698	238.29352	1.438741	35.044
5.	100	5.89408	234.91372	(1-5)- 11.67964	39.856

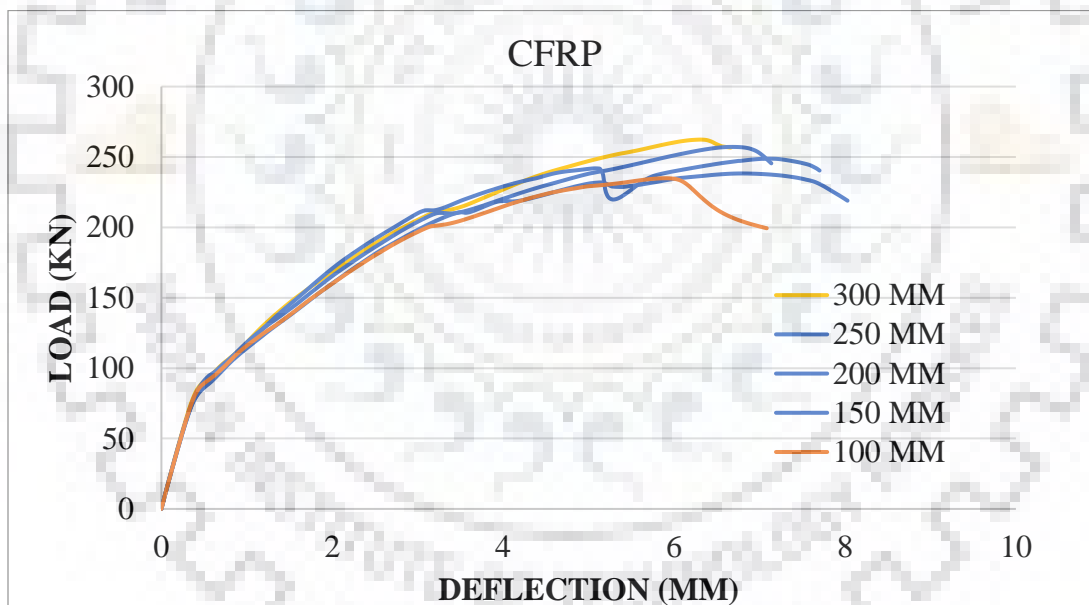


Fig. 5.14 Load v/s deflection curve of CFRP

Table 5.5 Load vs deflection data of BFRP and E-GFRP

S No.	Height (mm)	BFRP		Variation (%)	Secant stiffness	E-GFRP		Variation (%)	Secant stiffness
		Deflection	Load			Deflection	Load		
1.	300	6.35919	256.3016	4.482649	40.30	6.44438	248.254	2.761386	38.548
2.	200	6.94117	245.3054	5.336985	35.34	6.94588	241.583	4.826643	34.780
3.	100	5.90681	232.8768	(1-3)- 10.06	39.43	5.85527	230.460	(1-3)- 7.721	39.35

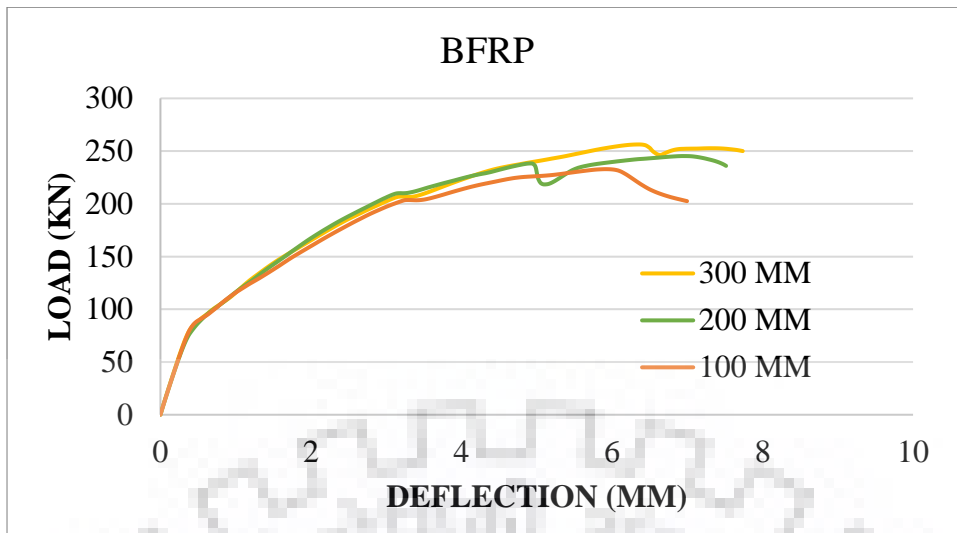


Fig. 5.15 Load v/s deflection curve of BFRP

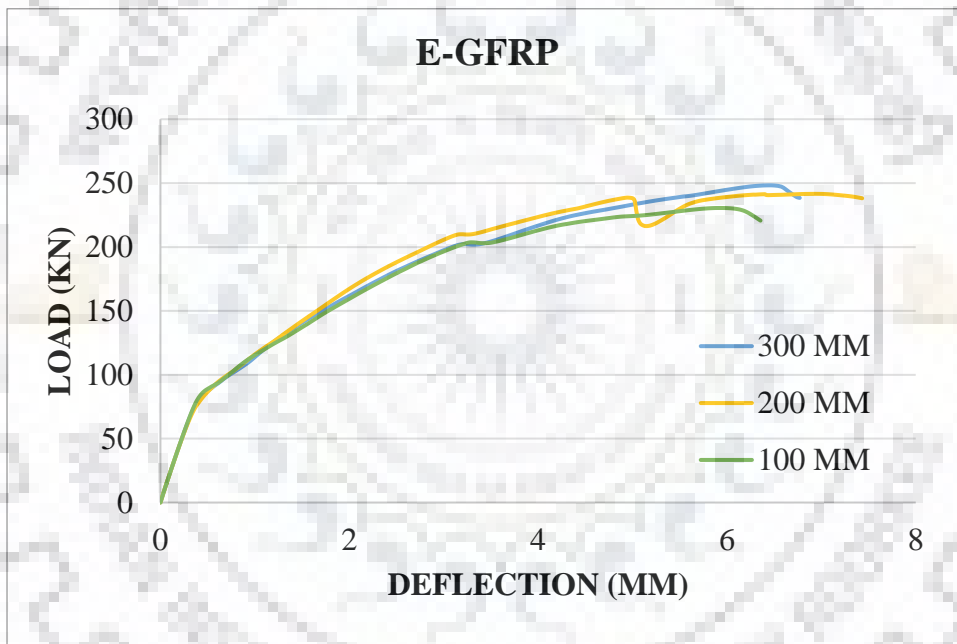


Fig. 5.16 Load v/s deflection curve of E-GFRP

In above case increasing height one-third (100mm) to full depth (300mm) capacity of beam increasing 11.68%, 10.06% and 7.8% respectively in case of CFRP, BFRP and E-GFRP.

According to Fig. 5.14 CFRP take higher result as compare to BFRP and E-GFRP. initially displacement is increasing up to two-third beam height of FRP laminate then after decreasing. So, at 100mm height more secant stiffness as compare 200mm height of CFRP laminate and maximum secant stiffness get at 300mm height.

In Fig.5.15 and 5.16 shows same behaviour between BFRP and E-GFRP.

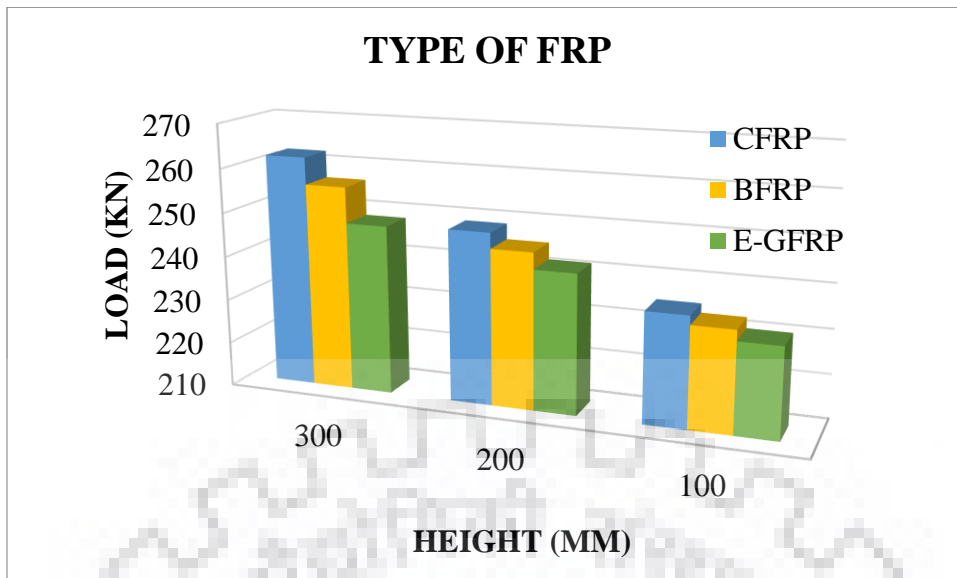


Fig. 5.17 Load v/s height curve of FRP with different type.

In below Fig. 5.17 shows that CFRP takes maximum load then BFRP then followed by E-GFRP. At one-third depth of beam FRP laminate approximately become equal difference, but at full depth of FRP laminate more gap become between BFRP and E-GFRP laminate as compare to CFRP and BFRP laminate.

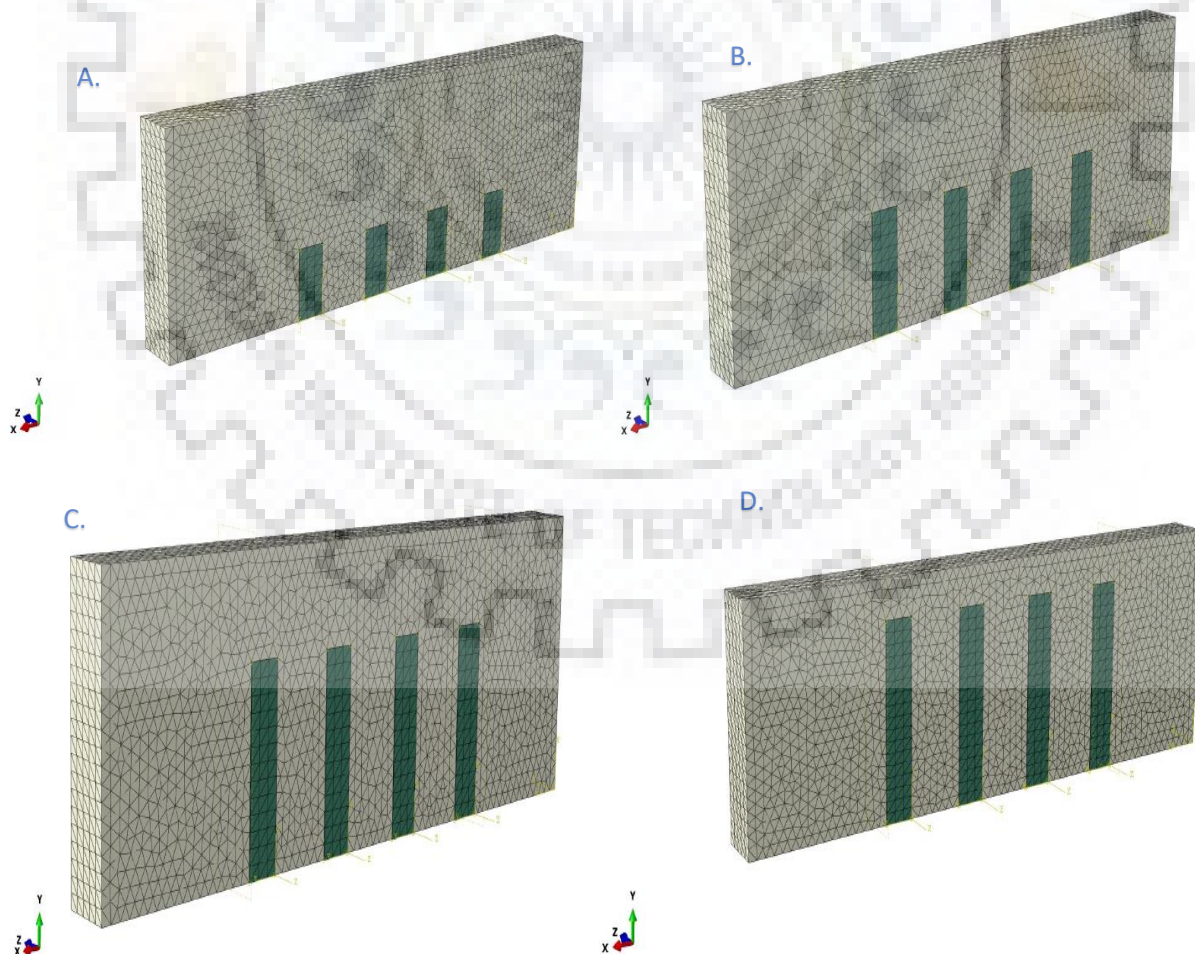


Fig. 5.18: Different heights of CFRP.

5.4.2 Orientation effect of CFRP

In case of orientation of CFRP study's 90° and 45° orientation of 1.2mm single layer FRP laminate. Both of the case induces fibre orientation concept in FEM model. Load vs deflection values with different height shown in Table 5.6

Table 5.6 Load vs deflection values with different height

S. No.	HEIGHT	90° Orientation		45° Orientation		% Change
		Deflection	Load	Deflection	Load	
1.	300	6.30268	262.3508	6.81797	251.11152	-4.47
2.	250	6.67515	257.15192	5.41011	256.2808	-0.34
3.	200	7.36457	241.67736	6.44419	261.4584	8.184
4.	150	6.80698	238.29352	6.45323	245.62314	3.0758
5.	100	5.89408	234.91372	7.1092	242.10718	3.0622

Since the shear crack propagates in the diagonal manner, therefore CFRP laminate is used at 45° orientation with longitudinal axis of RC beam.

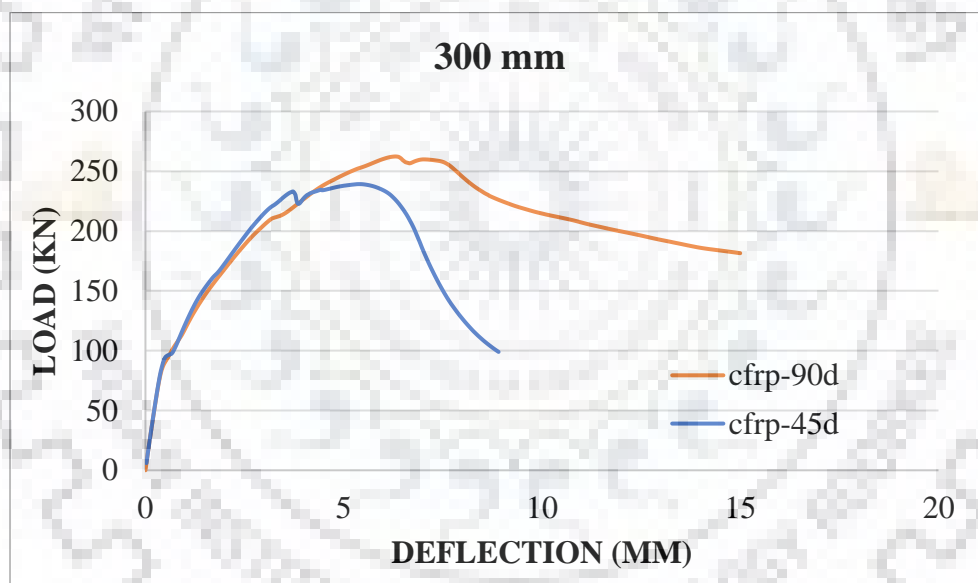


Fig. 5.19 Load vs deflection curve at 300mm height

In Fig.5.19, 45° orientation takes lesser load and deflection as compare to 90° orientation because at 45° debonding failure was occurred.

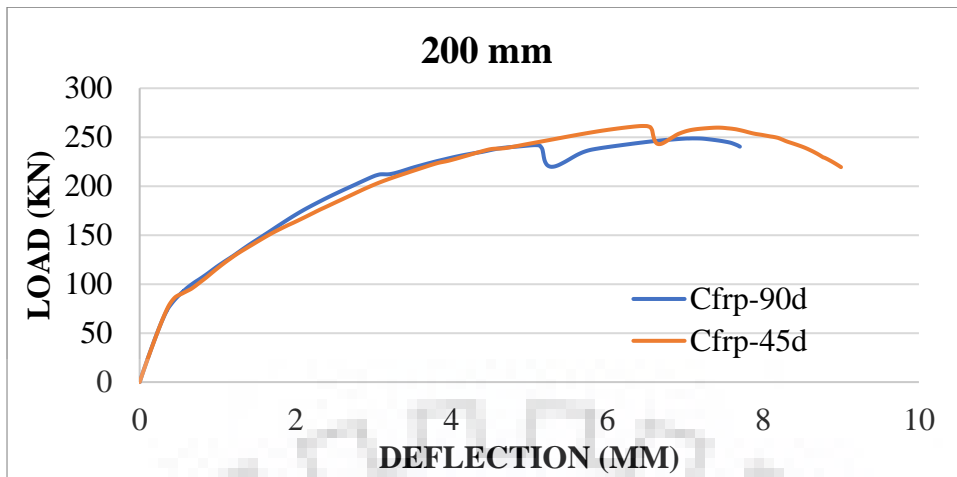


Fig. 5.20 Load vs deflection curve at 200mm height

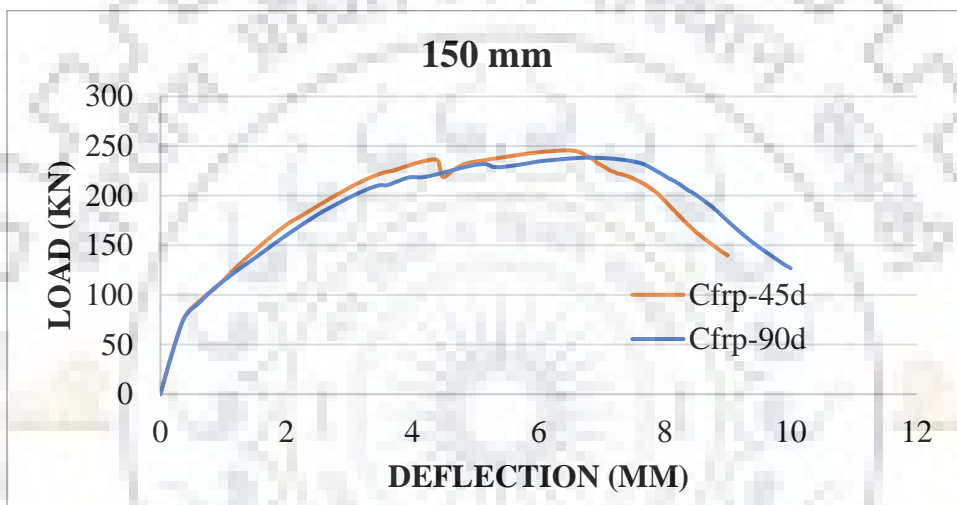


Fig. 5.21 Load vs deflection curve at 150mm height

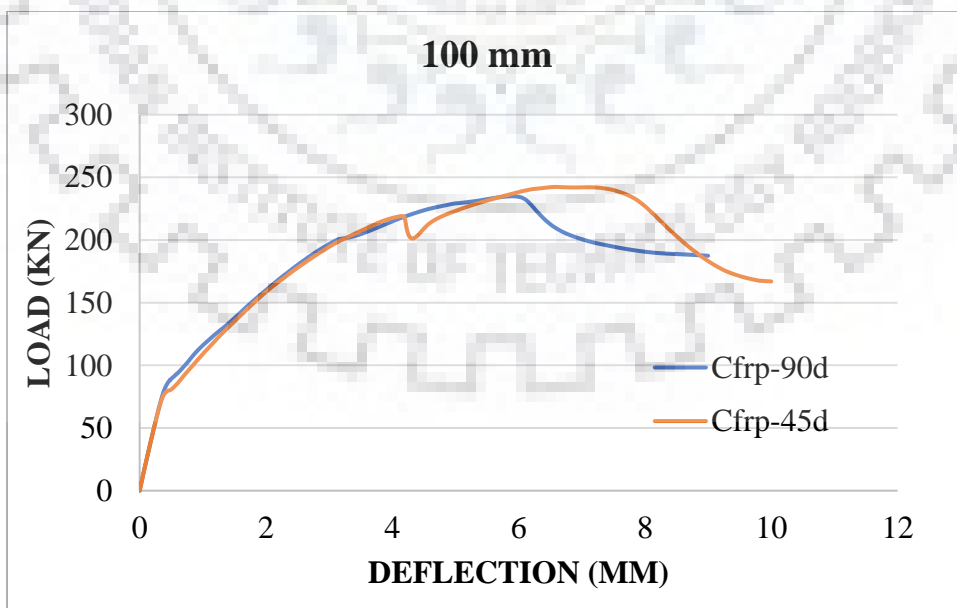


Fig. 5.22 Load vs deflection curve at 100mm height

In Fig. 5.20-5.22, up to two-third depth of beam take higher load at 45° orientation as compare to 90° orientation. Therefore at 45° ply was found to be better in resisting shear crack as compare to 90° orientation cross ply till two-third of beam after which its effect starts to decrease.

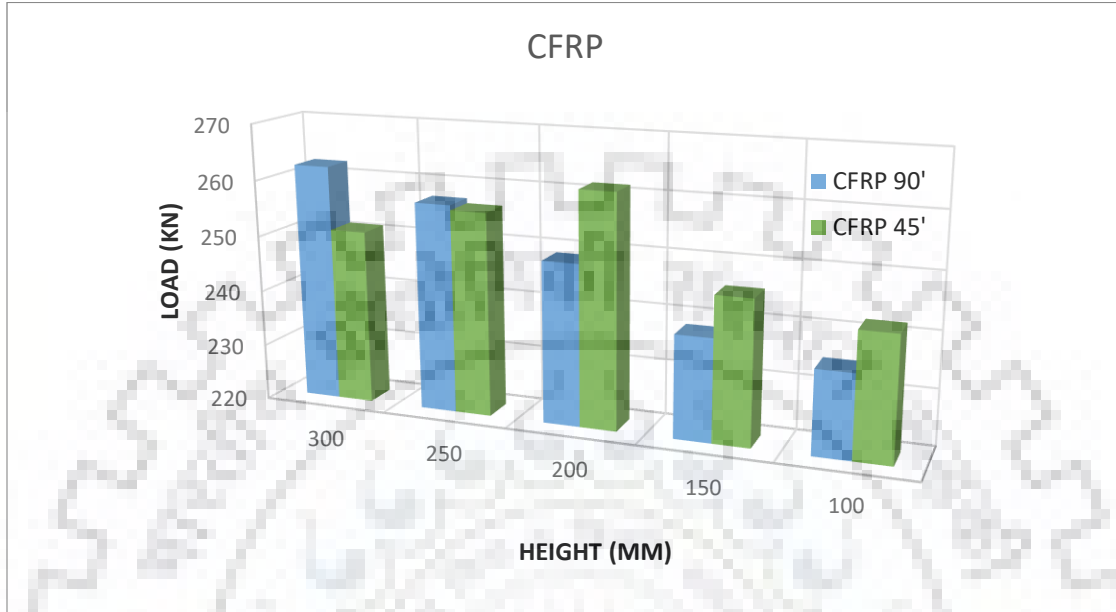


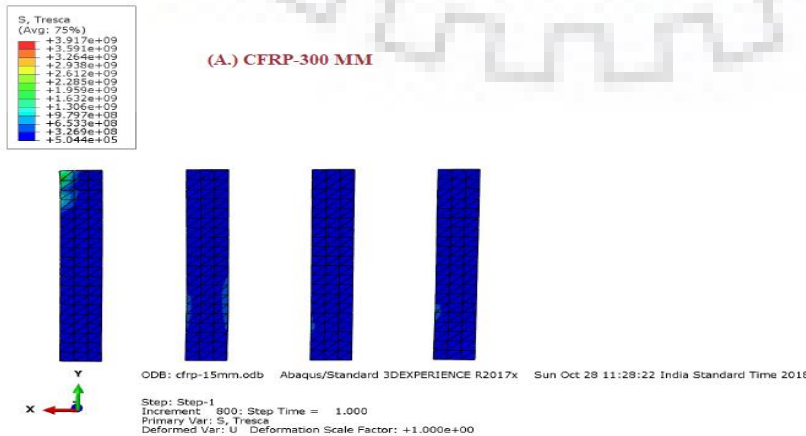
Fig. 5.23 Load vs height of different orientation.

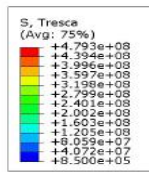
In above Fig.5.23, at 90° ply orientation when increasing height of CFRP laminate load carrying capacity increases respectively but in case of 45° ply orientation when height of laminate increase, then load carrying capacity increasing up to two-third beam then decreasing.

In comparison to both cases maximum load carrying capacity difference (8.184%) coming two-third beam and minimum load carrying capacity difference (-4.47%) become at full depth.

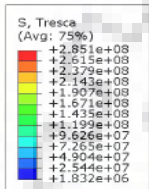
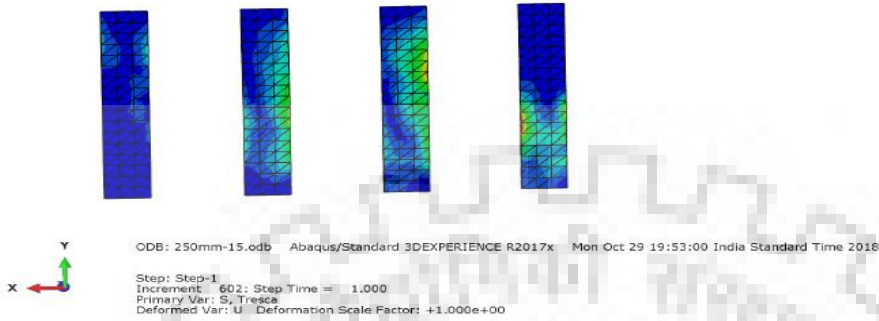
In Fig. 5.24 (A-E) shows Tresca stress variation of FRP plate at 90° orientation at different heights.

Printed using Abaqus/CAE on: Fri Apr 19 23:04:42 India Standard Time 2019

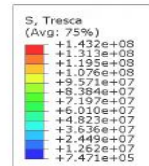
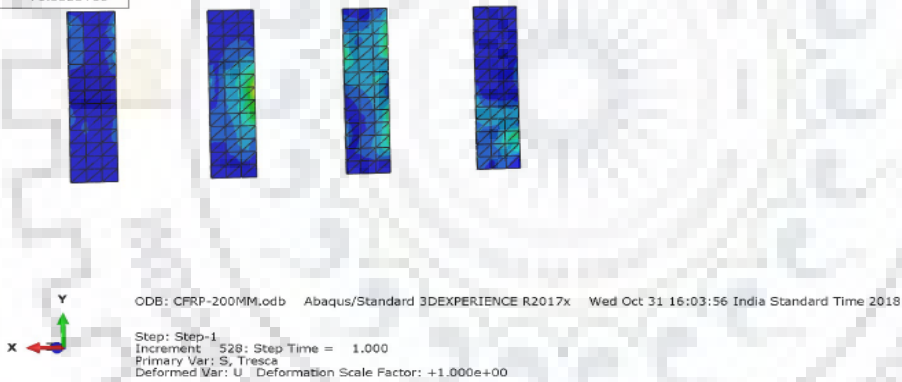




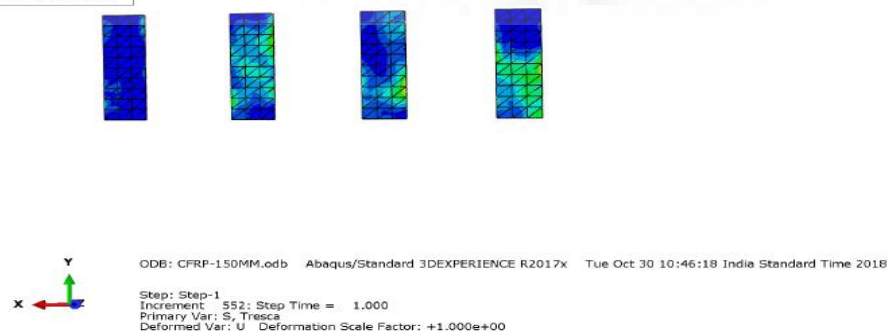
(B.) CFRP-250 MM



(C.) CFRP 200 MM



(D.) CFRP 150 MM



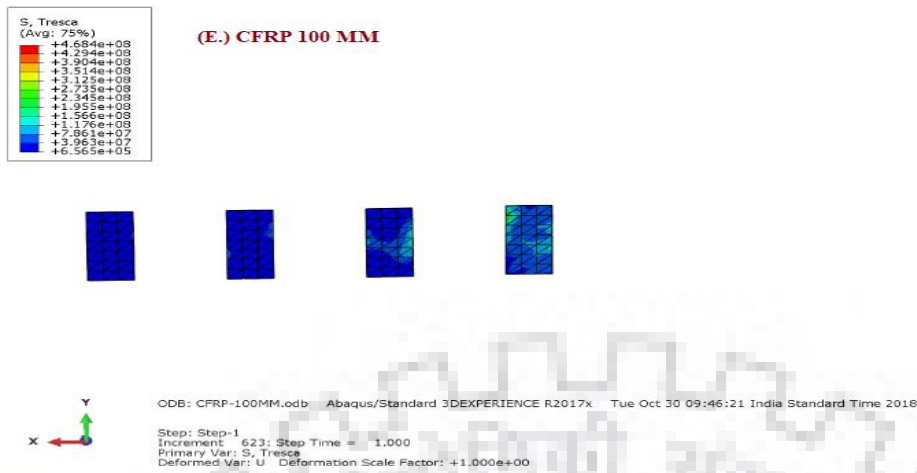
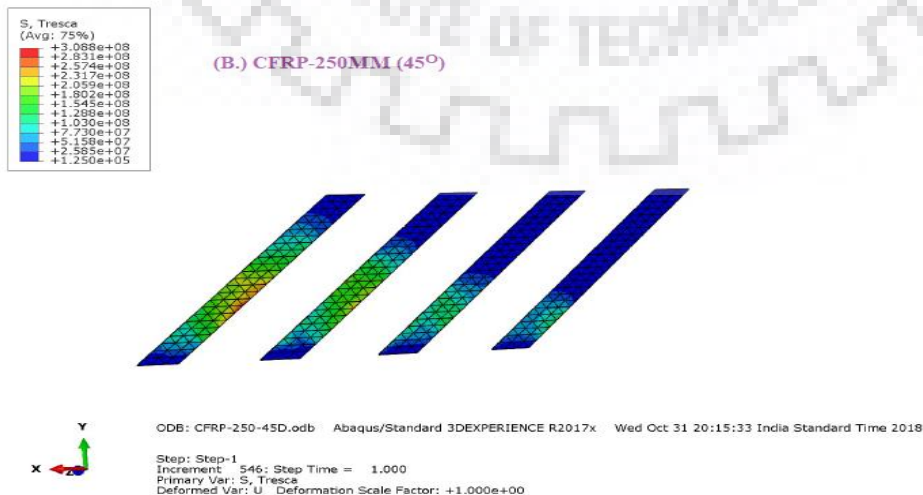
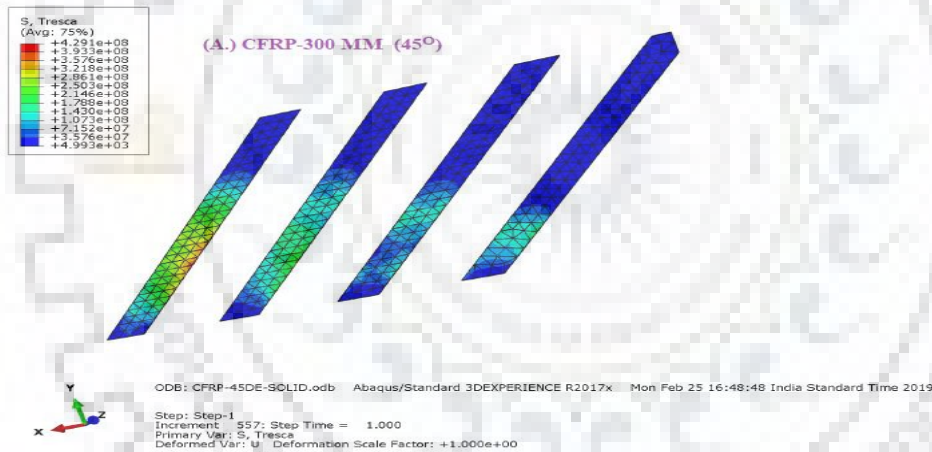


Fig. 5.24(A-E) Tresca stress variation of CFRP laminate at 90° orientation.

In below Fig. 5.25(A-E) shows Tresca stress variation of CFRP laminate at 45° orientation.



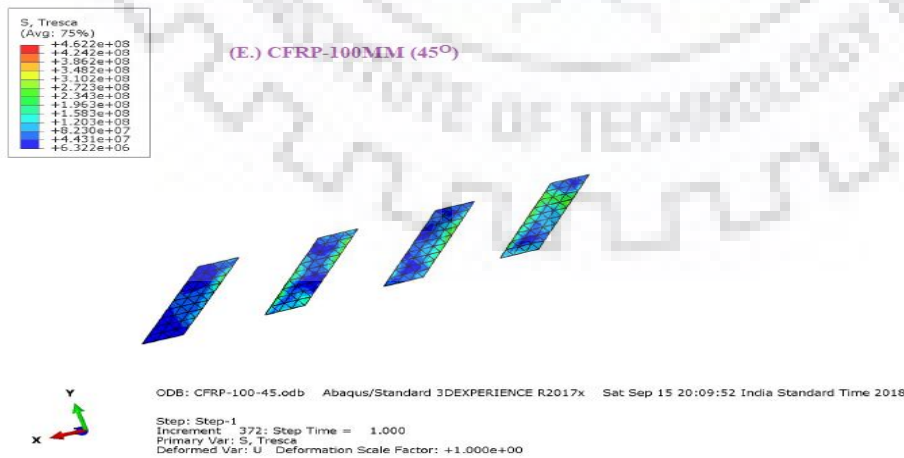
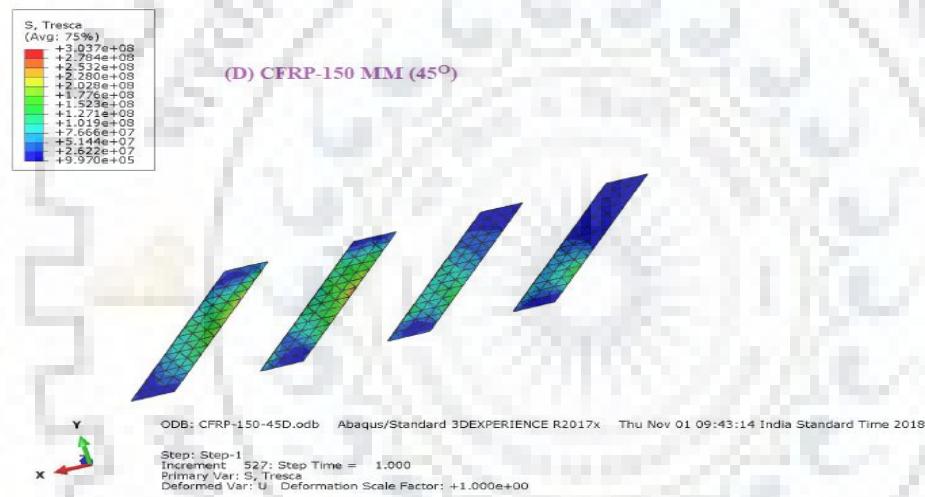
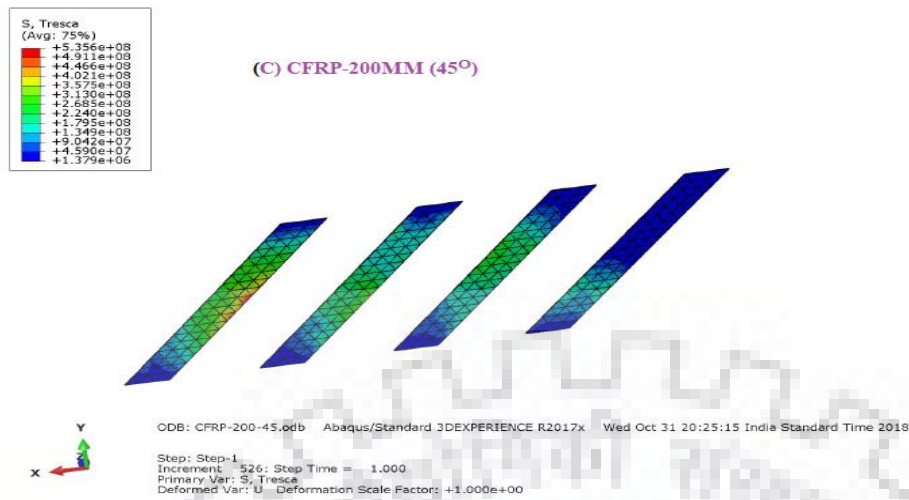


Fig. 5.25(A-E) Tresca stress variation of CFRP laminate at 45° orientation.

5.4.3 Effects in shear behaviour change of percentage tension reinforcement: -

In this section, change of tension reinforcement shows the variation of strengthened beam with respect to control beam. Detail comparative results are shown in Table 5.7

Table 5.7 Load vs deflection values in change of percentage of tension reinforcement

S.NO.	Bar Dia.	% of Steel	Control		CFRP		% variation
			Load	Displacement	Load	Displacement	
1.	14	0.68417	189.288	7.2398	214.431	7.2984	13.33
2.	16	0.8936	217.1557	7.71939	239.681	8.0768	10.37
3.	18	1.1309	230.5982	6.76094	262.3508	6.3027	13.77
4.	20	1.3962	236.2051	5.75595	265.557	5.8143	12.43
5.	25	2.1816	248.7128	4.50464	268.56	4.734	7.98
6.	32	3.5744	261.3761	3.5858	276.99	3.7818	5.98
% load increase			38.03%		29.18%		

Some general information of RC beam minimum percentage of tensile steel according to IS 456-2000

$$\frac{A_{st}}{bd} \times 100 = \frac{0.85}{f_y} \times 100$$

So, minimum percentage of tensile reinforcement = $\frac{0.85}{415} \times 100 = 0.205\%$

And maximum tensile reinforcement is 4% of the cross-section area, so in the above table selection range of percentage of tension reinforcement satisfy the above criteria.

According to IS456-2000 due to increase in percentage tensile reinforcement nominal shear strength (τ_c) also increases. So here more shear loads are taken by tensile reinforcement.

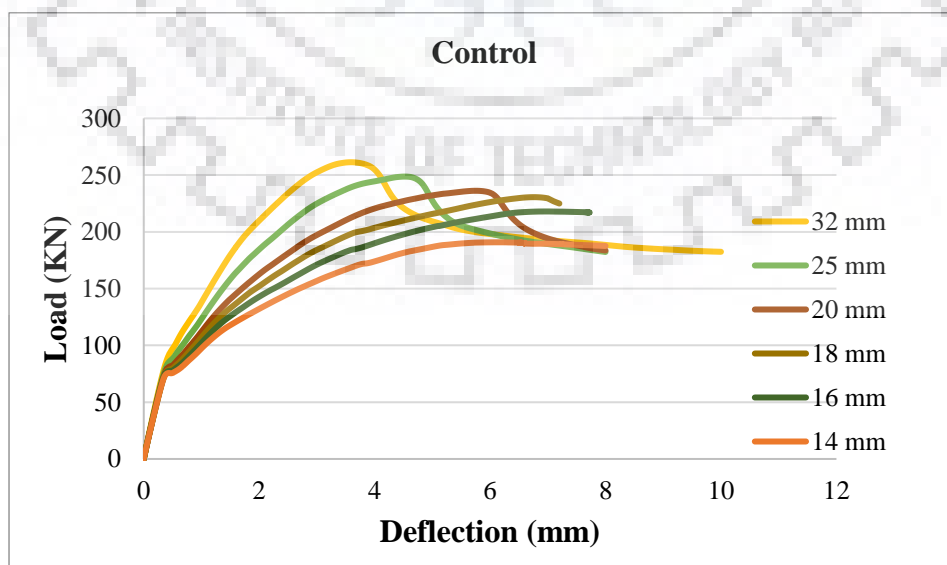


Fig. 5.26 Load vs deflection curve of control beam in change of percentage of steel

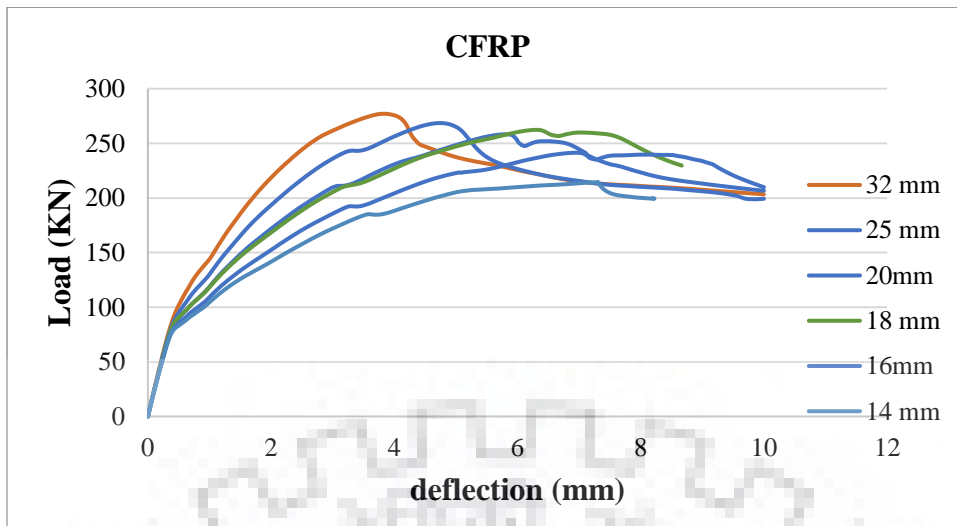


Fig. 5.27 Load vs deflection curve of CFRP strengthen beam in change of percentage of steel

In Fig.5.26 and 5.27, due to increase in the tensile reinforcement load carrying capacity also increased while the corresponding deflection decreased. In another term secant stiffness of RC strengthening beam was increased as it became stiffer and ductility decreased.

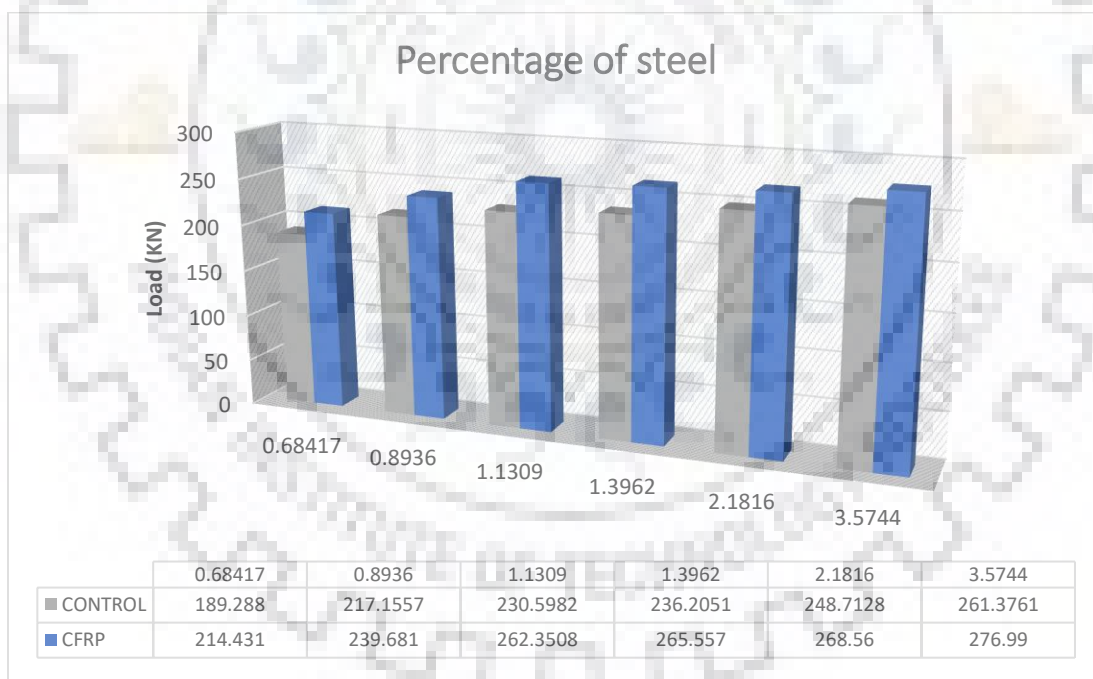


Fig. 5.28. Load vs percentage of steel chart compare control and CFRP strengthen beam.

According to Fig 5.28, in CFRP strengthened beam with respect to control beam strength variation increased up to 1.1309% of steel then it was decreased.

When percentage of steel increase from 0.68% to 3.57% in control beam variation of strength become 38.03%, but in case of CFRP strengthen beam variation became 29.08%.

Chapter -6

Conclusions and recommendations

6.1 Conclusion

FRP is the one of the best solutions to enhance the shear capacity of reinforced concrete beam. There is brittle failure in shear of RC beam, and the brittle failure is dangerous so shear strengthening is done to avoid shear failure. The objective of the present work was to solve this problem and to further study the effect of some parameters such as types of FRP laminate, orientation of FRP laminate, height of FRP laminate and percentage of tensile reinforcement. A non-linear three-dimensional FEM model was prepared on ABAQUS and successfully validated using the experimental results obtained from already published research papers.

The conclusive remarks of the parametric studies can be summarised as below:

- ❖ A 3D Finite element model has been developed using Abaqus to study the effect of shear strengthening of RC Beams using different types of FRP and different varying parameters.
- ❖ The results of three-dimensional FEM model have been validated with the some published experimental (Obaidat 2007) and finite element results (Obaidat 2010).
- ❖ CDP property has been proved to be quite efficient in numerical modelling the RC beam and it also successfully represent the stress strain behaviour of concrete under compression and tension.
- ❖ To achieve perfect results, orthotropic behaviour of FRP has been used and mechanical properties have been calculated with the **Rule of Mixture** and **Inverse Rule of Mixture**.
- ❖ In case of interface, the perfect bond model achieves little more ultimate strength as compare to cohesive bond model. When comparisons are made between solid and shell FRP models, shell composite model shows more strength as compared to single FRP solid layer. Perfect bonding does not show debonding failure but cohesive bond show debonding behaviour between concrete and FRP laminate layer.
- ❖ As the section secant stiffness of CFRP strengthened beam was increased with respect to the control beam, crack width of strengthened beam decreased. In both the cases, initial part takes higher stiffness and linear behaviour at preloading stage and then secant stiffness decreased at the time of failure.
- ❖ Increasing the height of FRP wrapping from one-third (100mm) to full depth (300mm), capacity of beam increased by 11.68%, 10.06% and 7.8% respectively in case of CFRP, BFRP and E-GFRP strengthened beams.

- ❖ Carbon fibre reinforced polymer takes higher load as compared to BFRP and followed by E-GFRP. Initially displacement increased up to two-third of beam height of FRP laminate then decreased.
- ❖ The advantages of BFRP are mainly due to eco-friendly properties as basalt fibres are produced directly from naturally occurring molten volcanic rocks.
- ❖ 45° orientation takes lesser load and deflection as compare to 90° orientation at 300 mm height of FRP laminate as may be at 45° orientation debonding failure would have happened.
- ❖ Therefore, 45° ply arrangement was found to be better in resisting shear crack as compared to 90° orientation cross ply till the length of wrapping is two-third of beam depth after which its effect starts to decrease.
- ❖ In comparison between 90° orientation and 45° orientation, the difference in the maximum load carrying capacity is 8.184% at length of wrapping at two-third of beam depth while the difference in the minimum load carrying capacity is (-)4.47% at wrapping up to full depth.
- ❖ In case of control and strengthened beam, due to increase in percentage of tensile reinforcement, load carrying capacity increased while the corresponding deflection decreased. In another term secant stiffness of RC strengthened beam increased and became stiffer with decrease in the ductility.
- ❖ In case of CFRP strengthened beam with respect to control beam variation of strength increased up to 1.1309% of steel then after strength was decreased.
- ❖ When percentage of steel increases from 0.68% to 3.57% in control beam variation of strength became 38.03%, but in case of CFRP strengthened beam variation became 29.08%.

6.2 Scope of future works

- ❖ Study on different environment effects such as temperature variation, fire, creep, and corrosion of strengthened RC beam using different types FRP.
- ❖ Further investigation may be done with different interface between concrete and FRP laminate such as cohesive and perfect.
- ❖ Hybrid study such as basalt and carbon fibre, basalt and glass fibre, carbon and glass fibre may be performed to get environmental and mechanical effects.
- ❖ Study with changes in the grades of concrete.